Journal of Environmental Management 397 (2026) 127920

Contents lists available at ScienceDirect

Journal of Environmental Management

journal homepage: www.elsevier.com/locate/jenvman

Research article

Source-resolved $PM_{2.5}$ oxidative potential predicts global mortality burden: A machine learning approach

Charles O. Esu [a], Kuk Cho [a,b,*]

[a] Department of Environmental Engineering, Pusan National University, 2, Busandaehak-ro 63beon-gil, Geumjeong-gu, Busan, 46241, Republic of Korea
[b] Institute of Environmental Studies, Pusan National University, Republic of Korea

ARTICLE INFO

Keywords:
Particulate matter toxicity
Redox activity
Environmental epidemiology
Health risk assessment
Emission control policies

ABSTRACT

Fine particulate matter ($PM_{2.5}$) oxidative potential (OP_v) is a crucial health metric, varying significantly by emission source. While concentration-response functions (CRFs) exist linking $PM_{2.5}$ mass to OP_v ($OP_v^{PM2.5}$), the lack of source-resolved OP_v (OP_v^{source}) CRFs limits accurate risk assessment globally. We developed global OP_v^{source} CRFs by integrating machine learning, statistical techniques, and comprehensive datasets of $PM_{2.5}$ concentrations, source apportionment (50 countries), and measured OP_v (>10,000 measurements in 29 countries). Our analysis revealed distinct intrinsic OP per unit mass (OP_m) for major sectors, ranking: energy (ENE) > transportation (TRO) > industry (IND) > agriculture and residential combustion (AGS + RCO). Applying these CRFs to 2017 $PM_{2.5}$ source data across 203 countries, we estimated the global average OP_v^{source} at 0.78 nmol min^{-1} m^{-3} (95 % CI: [0.39, 1.2]). ENE (33 %) and AGS + RCO (31 %) were predominant contributors globally, with substantial national variations. Poisson regression demonstrated that OP_v^{source} is a significantly stronger predictor of $PM_{2.5}$-attributable mortality than $PM_{2.5}$ concentration or $OP_v^{PM2.5}$. These findings establish source-resolved OP_v as a critical, more accurate metric for assessing mortality risks, supporting targeted air quality policies and interventions to mitigate $PM_{2.5}$ health burden.

1. Introduction

Ambient air pollution poses significant threats to human health through both chronic and acute exposure pathways, with mortality being established indicator for assessing these impacts. Exposure to elevated levels of fine particulate matter ($PM_{2.5}$) has been linked to millions of premature deaths worldwide annually (Lelieveld et al., 2015; McDuffie et al., 2021). To quantify these health risks, researchers have developed concentration-response functions (CRFs), including the integrated exposure-response (IER) model (Burnett et al., 2014) and the global exposure mortality model (GEMM) (Burnett et al., 2018). These CRFs synthesized data from multiple cohort studies across diverse global regions (Burnett et al., 2014, 2018; Liu et al., 2019). More recently, a study enhanced mortality predictions by focusing on source-specific $PM_{2.5}$ exposure (Zhang et al., 2023b) as emissions from anthropogenic source sectors (e.g., industry, energy, residential, agriculture, and transportation) may provide more stable relationships for health impact assessment compared to total $PM_{2.5}$ concentrations (Bates et al., 2015).

Oxidative potential (OP) has emerged as another indicator for assessing both chronic and acute health effects of $PM_{2.5}$ (Bates et al., 2019; Daellenbach et al., 2020). Oxidative stress arises from an imbalance between oxidants and antioxidants in the human respiratory system, potentially triggering various adverse health outcomes (Bates et al., 2019; Crobeddu et al., 2017; Lavigne et al., 2018; Liu et al., 2014; Strak et al., 2017). The dithiothreitol (DTT) assay, an acellular method for assessing OP, has proven particularly effective as an indicator of oxidative stress (Bates et al., 2019; Shiraiwa et al., 2017). Studies investigating the relationship between $PM_{2.5}$ OP and health outcomes have been conducted in various regions, including the United States (Abrams et al., 2017; Fang et al., 2016), European countries (Atkinson et al., 2016; Janssen et al., 2015), and China (He et al., 2021). While CRFs between reactive oxygen species and $PM_{2.5}$ concentration (Lakey et al., 2016) and between extrinsic OP (OP_v, i.e., per m^3 of air) and $PM_{2.5}$ concentration (Salana et al., 2024) have been explored, the development of globally representative CRFs linking OP_v directly to $PM_{2.5}$ sources remains limited by spatial coverage and data availability. This is despite growing datasets of $PM_{2.5}$ source concentrations and OP_v measurements across various locations (Aldekheel et al., 2024; Bates et al., 2019;

* Corresponding author. Department of Environmental Engineering, Pusan National University, 2, Busandaehak-ro 63beon-gil, Geumjeong-gu, Busan, 46241, Republic of Korea.
E-mail address: kukcho@pusan.ac.kr (K. Cho).

https://doi.org/10.1016/j.jenvman.2025.127920
Received 25 June 2025; Received in revised form 12 October 2025; Accepted 2 November 2025
Available online 3 December 2025

Bhattu et al., 2024; Daellenbach et al., 2020; Giannossa et al., 2022; Liu et al., 2018; Shang et al., 2022; Shen et al., 2022; Yao et al., 2024). Consequently, no study has yet reported globally applicable CRFs for specific $PM_{2.5}$ source sectors. This omission is significant, as source-specific CRFs could offer more accurate health risk assessments than those based on bulk $PM_{2.5}$, particularly given the substantial national variations in $PM_{2.5}$ source contributions.

To address this critical gap, we developed a global OP_v CRF for major anthropogenic $PM_{2.5}$ source sectors (OP_v^{source}) using machine learning (ML) and statistical modeling approaches. We derived these OP_v^{source} CRFs by analyzing two relationships: 1) OP_v versus $PM_{2.5}$ mass concentrations, resulting in total $PM_{2.5}$ OP CRF ($OP_v^{PM2.5}$) and 2) specific source concentrations versus $OP_v^{PM2.5}$. This analysis utilized extensive data, incorporating over 10,000 $OP_v^{PM2.5}$ measurements from 29 countries and more than 550 $PM_{2.5}$ source apportionment studies across 50 countries (spanning 1990–2022). The resulting OP_v^{source} CRFs demonstrated a reduced standard error compared to the $OP_v^{PM2.5}$ CRF and was rigorously validated ($R^2 = 0.95$) by measurement data. By integrating these OP_v^{source} CRFs with $PM_{2.5}$ exposure data and mortality estimates for 2017 (McDuffie et al., 2021), we assessed country-level oxidative burden, sector-specific contributions, and explored their correlation with $PM_{2.5}$-attributable mortality across 203 countries. The primary innovation of this study lies in the development of these OP_v^{source} CRFs, which offer enhanced precision relative to existing CRFs relating OP_v and total $PM_{2.5}$ concentration. Furthermore, OP_v^{source} exhibited a stronger and more significant association with $PM_{2.5}$-attributable mortality compared to both $PM_{2.5}$ mass and $OP_v^{PM2.5}$, underscoring the profound implication of our findings. These novel OP_v^{source} CRFs enable the estimation of source-specific OP_v from $PM_{2.5}$ source concentrations, offering a powerful tool for identifying key OP_v sources at local to global scales and ultimately informing more targeted and effective mitigation strategies.

2. Methods

2.1. $PM_{2.5}$ OP_v data collection

Fig. 1 shows the overall modelling workflow used in this study. In the first stage, we compiled $PM_{2.5}$ concentration and OP_v data from peer-reviewed studies. Our analysis focused on studies reporting OP_v measured via the DTT assay. From 70 publications (2003–2022), we extracted 10,659 $PM_{2.5}$ samples across 121 sampling campaigns in 152 urban areas, spanning 29 countries (14 European, 10 Asian/Middle Eastern, 3 North American, and 2 South American). For each study, we recorded mean $PM_{2.5}$ and OP_v concentrations, standard deviations, sample sizes, and temporal averaging scales (daily to annual). To ensure consistency, we standardized all measurements to μg/m^3 ($PM_{2.5}$) and nmol min^{-1} m^{-3} (OP_v). Studies reporting single measurements or insufficient sample replication were excluded to mitigate biases from unstandardized methodologies. The summary statistics of this data

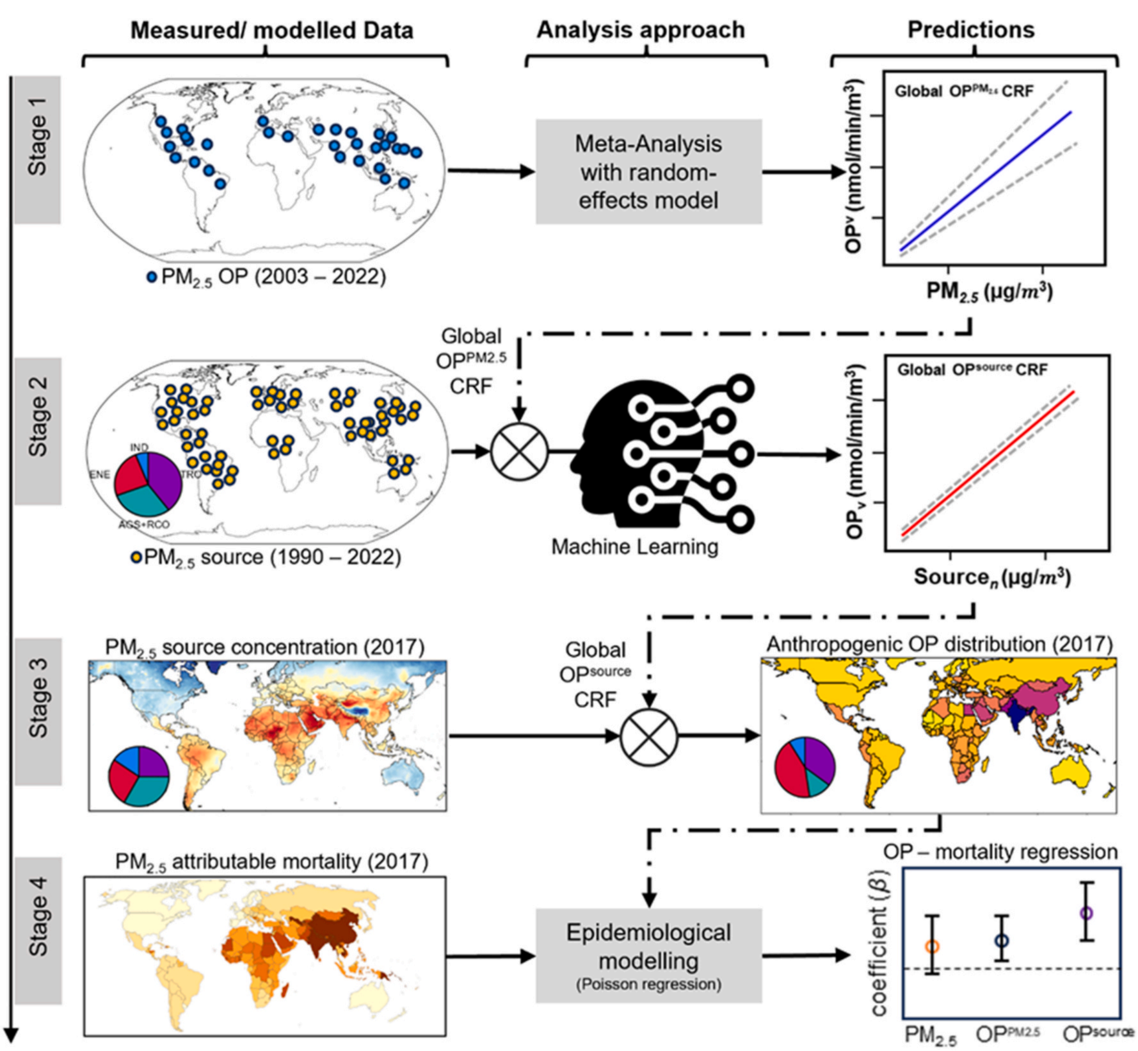

Fig. 1. | **Schematic of the modelling framework.** The diagram illustrates the key analytical steps, from initial data collection and processing, through the development of OP_v^{source} to the final estimation of global health effects.

including the countries covered and the data span is presented in Supplementary Table 15.

2.2. $PM_{2.5}$ source-sector concentration data collection

In the second stage, we synthesized $PM_{2.5}$ source-sector concentration data from published studies worldwide, which employed two primary methodologies: (1) Receptor modeling (e.g., positive matrix factorization (PMF), principal component analysis (PCA), and chemical mass balance (CMB)), which apportions sources based on measured chemical composition. (2) Chemistry transport models (CTMs), which estimate sectoral contributions via sensitivity analyses using emission inventories, validated against observational data (McDuffie et al., 2021; Zhang et al., 2023b). CTM studies focus on five primary anthropogenic sectors: industry (IND), agriculture (AGS), residential combustion (RCO), traffic (TRO), and energy generation (ENE) (definitions in Supplementary Table 8). Receptor models, while resolving finer source categories, often conflate sources with overlapping chemical profiles (Hopke et al., 2020). To ensure consistency, we harmonized receptor-derived sources into the five CTM-aligned sectors (Supplementary Table 9).

Data spanned 50 countries (1990–2022), with source-specific concentrations calculated by multiplying reported fractional contributions by total $PM_{2.5}$ levels. Studies lacking total $PM_{2.5}$ measurements or conflating key sources (e.g., biomass burning + vehicle) were excluded. Agriculture and residential combustion sectors (AGS + RCO) were merged due to shared biomass-burning components (e.g., agricultural residue/open-field burning and residential wood combustion) (Hopke et al., 2020). The summary statistics for local source apportionment data are presented in Supplementary Table 16.

2.3. Statistical and machine learning analysis for $PM_{2.5}$ OP_v ($OP_v^{PM2.5}$) and source-specific OP_v (OP_v^{source}) CRF

The global associations of $PM_{2.5}$ concentrations and OP_v ($OP_v^{PM2.5}$) was estimated using a meta-regression framework in stage 1 of Fig. 1, consistent with prior methodologies (Burnett et al., 2014, 2018; Liu et al., 2019; Zhang et al., 2023b). To account for heterogeneity across studies—stemming from variations in design and analytical methods—a random-effects model was applied, with OP_v as the dependent variable and the $PM_{2.5}$ concentration as the moderator. We then developed OP_v^{source} CRFs integrating the established $OP_v^{PM2.5}$ CRFs with the $PM_{2.5}$ source apportionment data within a ML framework using Feature Localized Intercept Transformed SHAP (FLIT-SHAP) (Esu et al., 2024) (Detailed in Supplementary Text 1 and summarized in stage 2 of Fig. 1). The analysis incorporated three key assumptions (Burnett et al., 2014; Zhang et al., 2023b): (1) oxidative stress, proportional to DTT consumption rates, serves as a proxy for $PM_{2.5}$ toxicity (Shiraiwa et al., 2017); (2) $PM_{2.5}$ and source-specific exposures exhibit linear relationships with OP_v within human exposure ranges; and (3) total OP_v reflects additive contributions from source-specific $PM_{2.5}$ mass, with no interactions. Model fitting was constrained to $PM_{2.5}$ concentrations within the observed global range (minimum to maximum averages). In stage 3 we combined OP_v^{source} CRFs with source sector concentrations at country and regional level for 2017 to obtain estimates of the global distribution of anthropogenic OP and the contribution of each source sector. Statistical analysis was performed in R using the *mgcv* and *meta* packages, with significance defined as $p < 0.05$ while ML workflows were implemented in Python.

2.4. Epidemiological modeling

Country-level associations between $PM_{2.5}$ properties (concentration, $OP_v^{PM2.5}$, OP_v^{source}) and all-cause mortality (2017) were assessed using generalized additive models with Poisson distributions, adjusted for overdispersion (Atkinson et al., 2016; Bates et al., 2015), summarized in stage 4 of Fig. 1. Mortality estimates in 2017, sourced from the 2019 Global Burden of Disease (GBD2019) study (Murray et al., 2020), were paired with population-weighted $PM_{2.5}$ and source-sector concentrations derived from GEOS-Chem simulations (McDuffie et al., 2021). Single-pollutant models evaluated individual $PM_{2.5}$ metrics, while multi-pollutant models concurrently assessed $PM_{2.5}$ concentration, $OP_v^{PM2.5}$, and OP_v^{source}. Standardized regression coefficients (β) and 95 % confidence intervals (CI) quantified variable importance, with higher β indicating stronger mortality associations. Spearman correlation complemented these analyses to evaluate monotonic trends. Statistical computations utilized Python's *statsmodels* package.

2.5. Uncertainty and model evaluation

To ensure the robustness of our modeling framework, we systematically evaluated both model performance and the propagation of predictive uncertainty. Model fit and stability were assessed using multiple complementary metrics: the Akaike information criterion (AIC), Bayesian information criterion (BIC), standard error (SE), and coefficient of determination (R^2). These metrics jointly balance explanatory power against model complexity, helping to avoid overfitting while ensuring reliable inference. To quantify predictive uncertainty, we explicitly accounted for input data variability at each modeling stage. In the $PM_{2.5}$-OP CRF, uncertainty was propagated through a random-effects meta-regression that incorporates the reported variance from each source study as a weighting factor. For the OP_v^{source}, uncertainty was captured via bootstrapping within the RF framework. This approach preserves the variability inherent in both the OP measurements and source apportionment estimates.

3. Results

3.1. Global $OP_v^{PM2.5}$ and OP_v^{source} CRFs

A meta-analysis was conducted using a global dataset $PM_{2.5}$ concentrations and OP measurements, encompassing various regions, seasons, and populations, to derive a global CRF for $OP_v^{PM2.5}$ (Fig. 2a). This analysis yielded a global average intrinsic OP of $PM_{2.5}$ ($OP_m^{PM2.5}$) estimated at 0.0254 nmol min^{-1} μg^{-1} (95 % CI: [0.0211–0.0297], p-value <0.0001, $R^2 = 0.56$; Supplementary Table 1; Supplementary Fig. 1). This statistically significant positive association indicates that OP_v increases with $PM_{2.5}$ concentration across a range of exposure. The linear CRF observed in this study aligns with findings from prior research demonstrating linear trends between measured OP_v and $PM_{2.5}$, even at low $PM_{2.5}$ concentrations (Salana et al., 2024; Shen et al., 2022). Similarly, prominent epidemiological studies investigating global $PM_{2.5}$ mortality risk, including the GEMM and others, have also reported linear or near-linear CRFs (Burnett et al., 2018; Schwartz et al., 2002; Weichenthal et al., 2016), although some acknowledge non-linear relationships for cause-specific mortality (Zhang et al., 2023b). The relatively wide CI and moderate R^2 value (0.56) for the $OP_v^{PM2.5}$ CRF are consistent with a previous continental-scale analysis that reported an R^2 of 0.39 for the regression of $PM_{2.5}$ concentration against OP_v (Salana et al., 2024). These observations suggest that variability in $PM_{2.5}$ composition likely contributes to differences in OP_v at equivalent $PM_{2.5}$ concentration. While acknowledging this inherent complexity of air pollution, these results underscore the potential of source-specific CRFs to provide a more refined understanding.

To develop source-resolved OP CRFs (OP_v^{source}; Fig. 2b), we integrated $PM_{2.5}$ source sector concentrations with the derived $OP_v^{PM2.5}$ CRF, employing ML techniques with FLIT-SHAP(Esu et al., 2024). Among various ML models tested (Supplementary Table 2), the Random Forest (RF) model exhibited the best performance, achieving an R^2 of 0.83 and a MAE of 0.38 nmol min^{-1} m^{-3} after hyperparameter optimization (Supplementary Table 3). The optimized RF model was subsequently used for FLIT-SHAP analysis to quantify the contribution of each source sector to OP_v. Linear CRFs for each source sector were then derived by

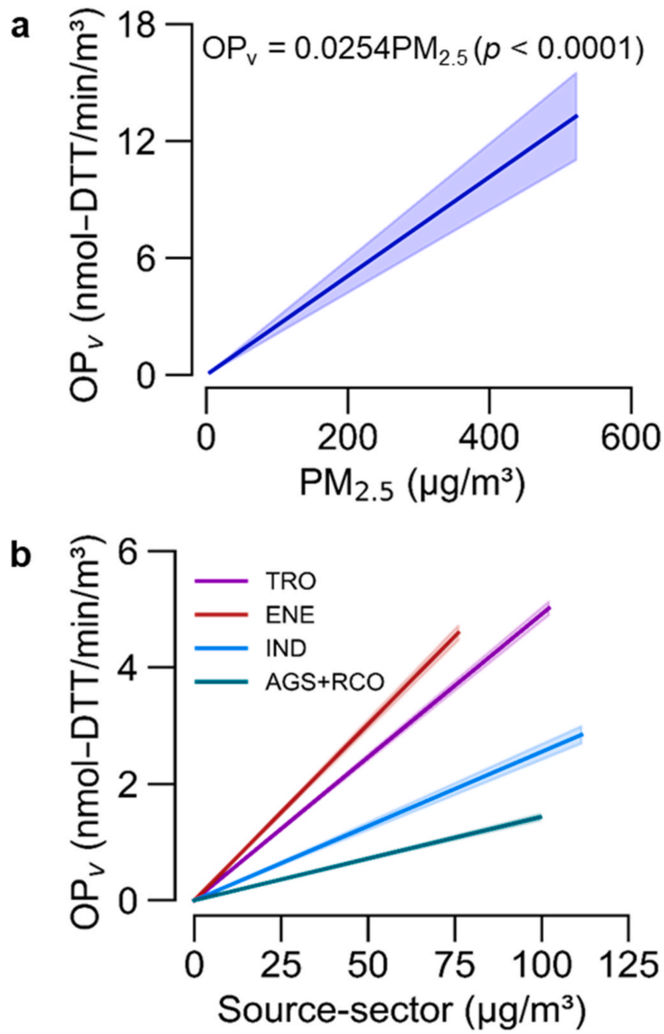

Fig. 2. | **Concentration-response functions for OPv across PM2.5 exposure range. (a)** Global $OP_v^{PM2.5}$ CRF derived from a meta-analysis of $PM_{2.5}$ concentrations and OP measurements (DTT assay) across 29 countries (n = 10,659 samples) from 2003 to 2022. **(b)** Global anthropogenic source-specific $PM_{2.5}$ OP (OP_v^{source}) CRFs from panel (a) with $PM_{2.5}$ source apportionments data from 50 countries (n = 590 cases) from 1990 to 2022, using the FLIT-SHAP explainable ML tool. Shaded areas in both panels represent 95 % CIs.

fitting linear relationships to the contribution estimates obtained from the FLIT-SHAP analysis (Fig. 2b, Supplementary Fig. 2). Both individual source sector OP_v^{source} CRFs and the combined OP_v^{source} CRF (Eq. (1)) demonstrated improved statistical quality compared to the $OP_v^{PM2.5}$ CRF, as indicated by metrics such as AIC, BIC, standard error and R^2, and further supported by uncertainty analysis for each model (Supplementary Table 4). Detailed fitting statistics for each source sector are presented in Supplementary Table 5. The slope of the OP_v^{source} CRFs, representing the OP_m^{source}, followed a descending order: Energy production (ENE): 0.060 (95 % CI: [0.059–0.062]) nmol min^{-1} µg^{-1} source > Transportation (TRO): 0.049 (95 % CI: [0.048–0.050]) > Industry (IND): 0.026 (95 % CI: [0.024–0.027]) > Agriculture and Residential (AGS + RCO): 0.014 (95 % CI: [0.014–0.015]), with all slopes statistically significant (p-value <0.0001).

$$OP_v^{source} = 0.060ENE + 0.049TRO + 0.026IND + 0.014(AGS + RCO) \quad (1)$$

To visualize the spatial distribution of OP_v, we calculated average OP_v^{source} values across countries (Fig. 3). Normalized sector contributions are further detailed in Supplementary Fig. 3. Globally, the average OP_v was estimated at 1.4 ± 1.24 nmol min^{-1} m^{-3}, with sectorial contributions of 39 % from ENE, 33 % from TRO, 9 % from IND, and 19 % from AGS + RCO.

Countries exhibiting the highest OP_v^{source} were Pakistan (3.29 ± 1.11 nmol min^{-1} m^{-3}), Mongolia (2.58 nmol min^{-1} m^{-3}), India (2.50 ± 1.51 nmol min^{-1} m^{-3}), China (2.38 ± 1.06 nmol min^{-1} m^{-3}), and Bangladesh (2.11 ± 0.74 nmol min^{-1} m^{-3}). In most of these top-ranked countries, TRO and ENE sectors were the dominant contributors to OP_v^{source}, with the exception of Bangladesh, where IND (54 %) and TRO (23 %) were the primary sources. Notable OP_v^{source} estimates from countries lacking prior measurements include Saudi Arabia (1.82 ± 0.96 nmol min^{-1} m^{-3}), Nigeria (1.56 ± 1.25 nmol min^{-1} m^{-3}), Poland (0.93 ± 0.36 nmol min^{-1} m^{-3}), and Australia (0.30 ± 0.28 nmol min^{-1} m^{-3}; Fig. 3, Supplementary Table 13).

3.2. Estimate of regional- and national-level OP_v^{source} for 203 countries in 2017

To estimate OP_v^{source} across all countries, a task not feasible with our data collection limited to 50 countries, we utilized population-weighted mean (PWM) source-specific $PM_{2.5}$ concentrations for 203 countries in 2017, as derived from a chemical transport model (McDuffie et al., 2021). These $PM_{2.5}^{source}$ data were integrated with our combined OP_v^{source} CRFs (Eq. (1)) to calculate national and regional OP_v^{source} and the contributions from various source sectors (Figs. 4 and 5).

Globally, we estimated an oxidative burden of 0.78 nmol min^{-1} m^{-3} (95 % CI: [0.39–1.2] nmol min^{-1} m^{-3}) attributable to annual ambient $PM_{2.5}$ exposure from anthropogenic sources in 2017 (Fig. 5b). The primary contributors to this global oxidative burden were ENE at 33 % and AGS + RCO at 31 %, followed by TRO at 20 % and IND at 16 % (Fig. 5c). At the regional level, Fig. 5b presents OP_v^{source} values for 21 world regions in descending order, revealing a trend similar to that of $PM_{2.5}$ concentration, though not identical. Sector-specific contributions, detailed in Fig. 5c, highlight distinct regional patterns. Notably, IND was the dominant contributor in Southern Latin America, driven largely by trends in Brazil and Peru (Fig. 4). ENE predominated in Southern Africa, Eastern Europe, North Africa and Middle East, Central Asia, and Central Europe. In contrast, AGS + RCO were the leading sources in Central Sub-Saharan Africa, Oceania, Western Sub-Saharan Africa, and Eastern Sub-Saharan Africa, while TRO made significant contributions in Western Europe and North America.

To elucidate localized drivers of OP_v^{source}, we analyzed country-level contributions, which provide insights more relevant to national contexts than global or regional aggregates. Pie charts in Fig. 4 illustrate the relative contributions of source sectors for the selected countries, with national-level results for 203 countries depicted in the central map of Fig. 4. Absolute OP_v^{source} values for select countries are shown above the pie charts. The highest OP_v^{source} levels were observed in India (1.74 nmol min^{-1} m^{-3}, 95 % CI: [0.85–2.69]) and Nepal (1.56 nmol min^{-1} m^{-3}, 95 % CI: [0.73–2.44]). These values are 5–9 times greater than those in countries such as the United States (0.19 nmol min^{-1} m^{-3}), the United Kingdom (0.23 nmol min^{-1} m^{-3}), Switzerland (0.24 nmol min^{-1} m^{-3}), Germany (0.29 nmol min^{-1} m^{-3}), Japan (0.29 nmol min^{-1} m^{-3}), and Italy (0.34 nmol min^{-1} m^{-3}). This disparity underscores the elevated health risks associated with $PM_{2.5}$ exposures.

Source contributions exhibited considerable variability across countries. ENE ranges from 7.7 % in Peru to 71.4 % in Qatar, while AGS + RCO varied from 3.6 % in Qatar to 49.4 % in Nigeria. TRO contributions spanned 11.9 % in Mongolia to 39.5 % in Italy, and IND contributions ranged from 6.0 % in Nigeria to 44.8 % in Peru. In absolute terms, ENE displayed the greatest variability, with OP_v^{source} ranging from 0.00069 to 0.95 nmol min^{-1} m^{-3}, followed by AGS + RCO (0.00066–0.67 nmol min^{-1} m^{-3}), TRO (0.0038–0.36 nmol min^{-1} m^{-3}), and IND (0.00015–0.31 nmol min^{-1} m^{-3}). These ranges indicate that ENE, followed by AGS + RCO, are the most variable contributors to OP_v^{source} globally. This variability often reflects national economic profiles, with oil producing countries typically exhibiting high ENE contributions and the

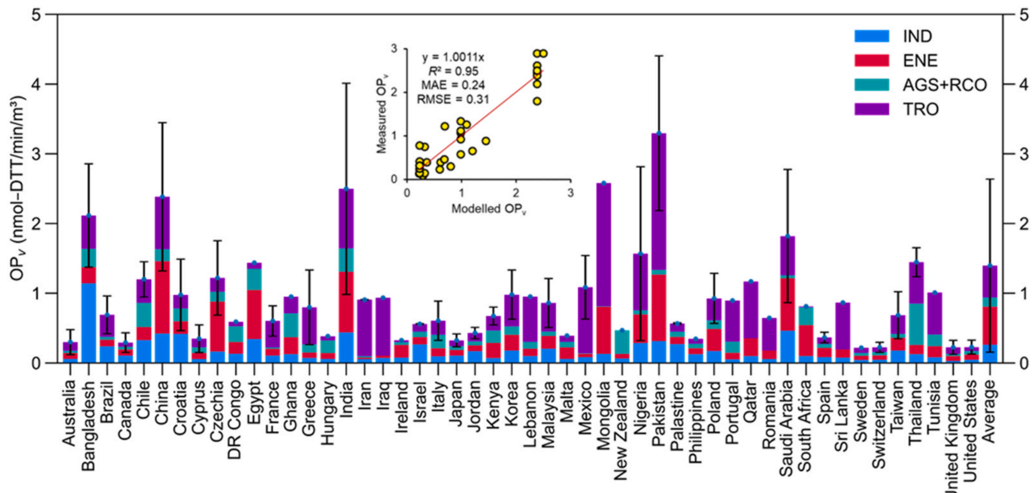

Fig. 3. | **Predicted country-level OP_v^{source} and validation to the measurements.** OP_v^{source} values were calculated for individual countries using the data mentioned in Fig. 2b. Values represent country-average OP_v^{source} within each country's source apportionment period. The bar labeled "Average" depicts the global average OP_v for each source sector, calculated across all countries and the entire period. Error bars indicate the standard deviation of OP_v^{source} estimates. Energy and transportation sectors are identified as the dominant contributors to OP_v globally. **Inset**: Comparison between estimated and measured OP_v at various locations (details in Supplementary Table 12).

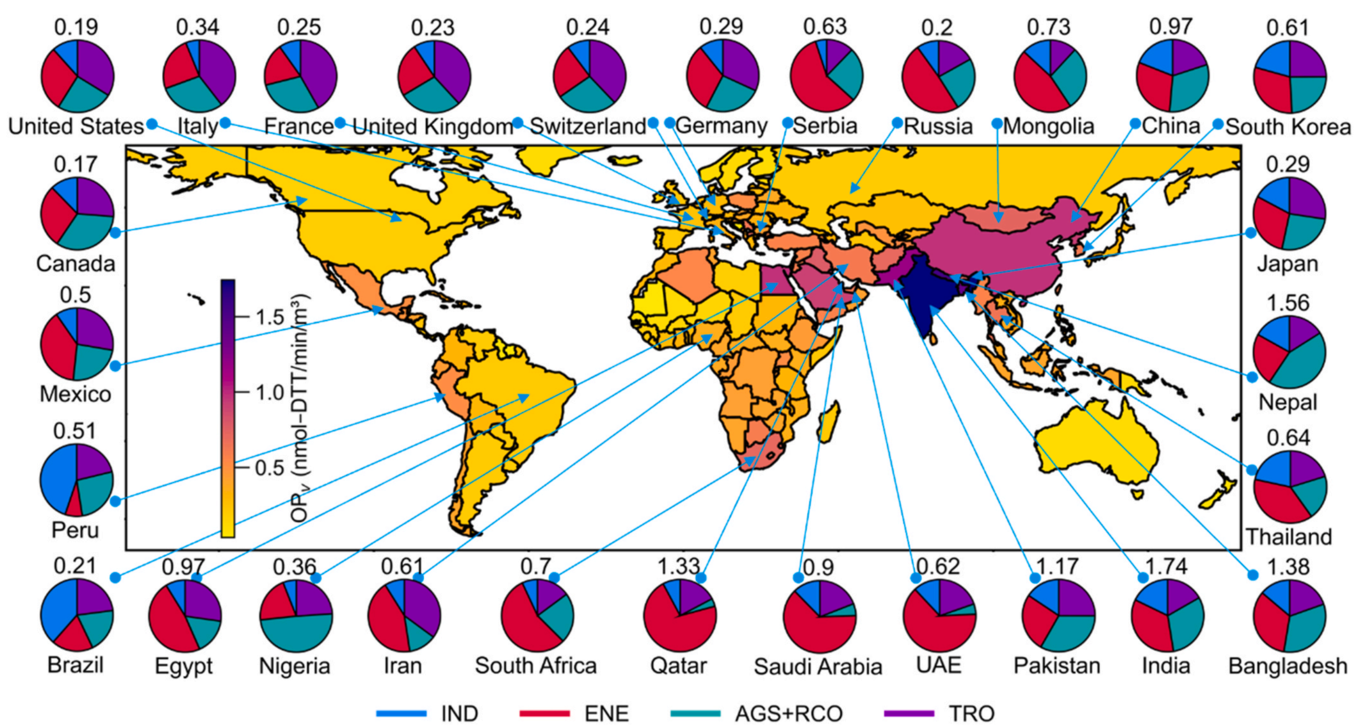

Fig. 4. | **Global oxidative burden from anthropogenic sources and fractional contributions by sector in 2017.** Map: National-level OP_v, calculated using our OP_v^{source} CRFs and PWM source-specific $PM_{2.5}$ concentrations for 2017 from McDuffie et al. (2021). Pie charts display the national annual average OP_v exposure (nmol min^{-1} m^{-3}; top of charts) and the fractional contributions from source sectors. Sectors include: Industry (IND): Industrial coal/non-coal combustion, and solvents; Energy (ENE): Energy production from coal and non-coal combustion; Transportation (TRO): Road, non-road, and international shipping; Agriculture and residential combustion (AGS + RCO): Residential and commercial combustion, agricultural waste burning, and open fires (see Supplementary Table 9 for details).

agrarian economies showing elevated contributions from AGS + RCO.

3.3. Association between 2017 national-level OP_v^{source} and mortality for 203 countries

We investigated a relationship using national-level PWM $PM_{2.5}$ concentration, $OP_v^{PM2.5}$, and both individual and combined OP_v^{source} for 2017 as independent variables, with estimated mortality using the GBD 2019 CRFs serving as the dependent variable. Initial trend analysis using spearman correlation indicated a stronger association between OP_v^{source} and mortality across all countries compared to $OP_v^{PM2.5}$, with correlation coefficients of $\tau = 0.62$ and 0.43, respectively (Fig. 6a). Cross-sectional analyses employing Poisson regression, a generalized linear model, further revealed positive associations between each of $PM_{2.5}$, $OP_v^{PM2.5}$, and OP_v^{source} and mortality in single pollutant models (Fig. 6b). The standardized estimate of coefficient (β) followed this order: OP_v^{source}: 1.30 (95 % CI: [1.16–1.43]]; $OP_v^{PM2.5}$ = $PM_{2.5}$: 0.93 (95 % CI: [0.79–1.07]). However, in a three-pollutant model incorporating $PM_{2.5}$,

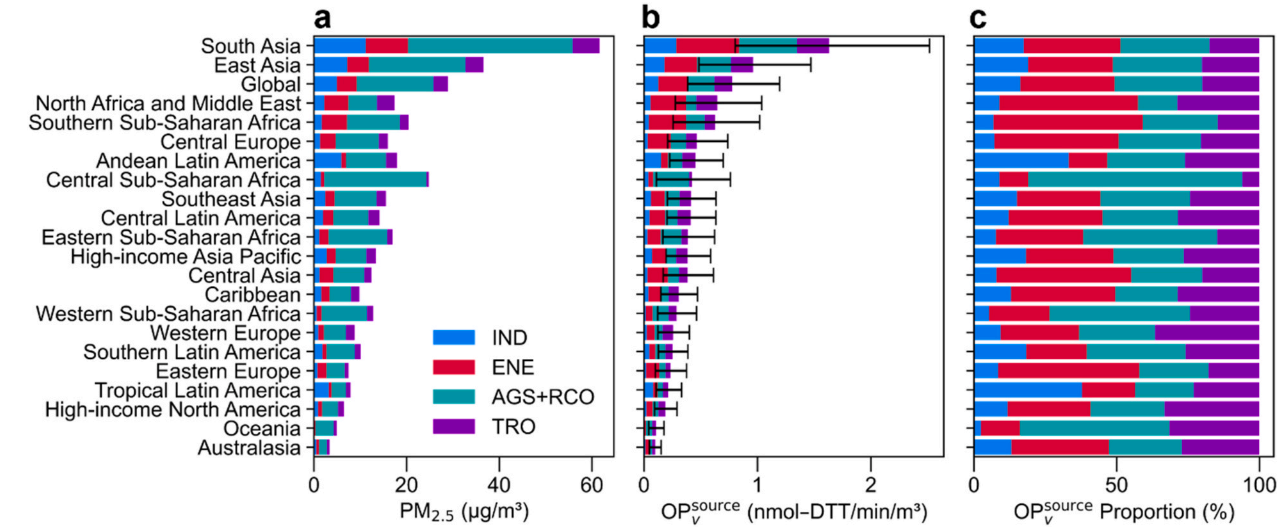

Fig. 5. | **Regional OPv and sectorial contributions across 21 world regions in 2017. (a)** PWM source-specific $PM_{2.5}$ concentrations for 2017, as provided by McDuffie et al. (2021). **(b)** Corresponding annual mean OP_v^{source} concentrations for each sector, with 95 % CIs. **(c)** Normalized sectoral contributions to OP_v^{source}.

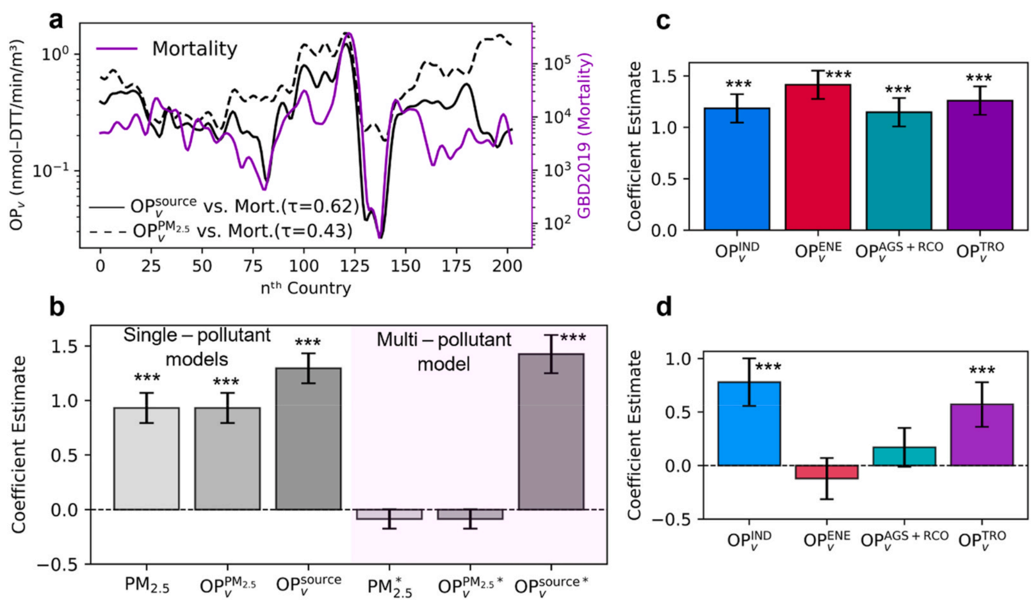

Fig. 6. | **Association between OP_v^{source} and mortality across 203 countries in 2017. (a)** Spearman correlation (τ) between OP_v^{source} (solid black line, left *y*-axis), $OP_v^{PM2.5}$ (dashed black lines, left *y*-axis), and mortality (purple line, right *y*-axis), with both *y*-axis on a log scale. Mortality data are calculated using the GBD 2019 CRFs as adopted from McDuffie et al. (2021). Poisson regression for **(b)** single- and multi-pollutant models using $PM_{2.5}$ mass, $OP_v^{PM2.5}$, and OP_v^{source}, for **(c)** single-pollutant models for source-specific OP_v (IND, ENE, AGS + RCO, and TRO), and for **(d)** multi-pollutant model including all source-specific OP_v variables as predictors for mortality. In panels (b), (c), (d), bars represent standardized coefficients (β), and lines indicate 95 % CIs. Significance levels are denoted as: $^*P < 0.05$; $^{**}P < 0.01$; $^{***}P < 0.001$.

$OP_v^{PM2.5}$, and OP_v^{source} simultaneously, only OP_v^{source} retained a significant association with mortality (β = 1.43, 95 % CI: [1.25–1.6]), while $PM_{2.5}$ and $OP_v^{PM2.5}$ showed no significant effects (Fig. 6b). This finding suggests that the CRFs developed for OP_v^{source} in this study may offer greater predictive power for mortality than $PM_{2.5}$ concentration or $OP_v^{PM2.5}$ alone.

To identify which source sector contributed most to mortality, we examined individual OP_v^{source} in single pollutant models. The standardized β were ranked as follows: ENE: 1.41 (95 % CI: [1.28–1.55]); TRO: 1.26 (95 % CI: [1.12–1.40]); IND: 1.18 (95 % CI: [1.05–1.32]); AGS + RCO: 1.15 (95 % CI: [1.00–1.28]) (Fig. 6c). In a multi-pollutant model including all source sectors, only OP^v from IND and TRO demonstrated significant association with mortality, with β = 0.78 (95 % CI: [0.56–1.00]) and β = 0.57 (95 % CI: [0.36–0.78]), respectively (Fig. 6d). Model summaries, including both unstandardized and standardized coefficients, are provided in Supplementary Tables 6 and 7, respectively. In this section, we emphasize standardized coefficients to ensure unbiased β estimates. Additionally, Spearman correlation trends between individual OP_v^{source} and mortality are presented in Supplementary Fig. 4.

4. Discussions

4.1. *Global OP_v CRFs for $PM_{2.5}$ and anthropogenic sources*

We presented a comprehensive and quantitative estimation of global

$OP_v^{PM2.5}$ and OP_v^{source} CRFs, which are critical for understanding the oxidative burden imposed by $PM_{2.5}$ on a global scale and for informing strategies to mitigate its associated health effects. Our $OP_m^{PM2.5}$ estimate of 25.4 pmol min^{-1} μg^{-1} $PM_{2.5}$ (95 % CI: [21.1, 29.7]) aligns with global ranges reported in prior studies (between 10 and 80 pmol min^{-1} μg^{-1}) (Shiraiwa et al., 2017). Post-2018 regional values further corroborate this consistency: China (24.3 ± 13.3, 27.86 ± 3.19 pmol min^{-1} μg^{-1}) (Deng et al., 2022; Xing et al., 2023); India (29.4 ± 18.48, 27.5 ± 5.8 pmol min^{-1} μg^{-1}) (Li et al., 2024; Puthussery et al., 2022); South Korea (27.5 ± 11.8 pmol min^{-1} μg^{-1}) (Kim et al., 2024); Japan (22.6 ± 16.8 pmol min^{-1} μg^{-1}) (Kurihara et al., 2022); Greece (27.98 ± 14.42 pmol min^{-1} μg^{-1}) (Paraskevopoulou et al., 2019); Denmark, Finland, and France (14–19 pmol min^{-1} μg^{-1}) and Canada (11.9 ± 7.46 pmol min^{-1} μg^{-1}) (Weichenthal et al., 2021). A detailed comparison is available in Supplementary Table 10. Additionally, a recent inter-continental study reported $OP_m^{PM2.5}$ values of 20 pmol min^{-1} μg^{-1} (Salana et al., 2024), reinforcing the global application of our model. However, notable deviations exist, with values as low as 5 pmol min^{-1} μg^{-1}) in Canada (Weichenthal et al., 2019) and as high as 60–190 pmol min^{-1} μg^{-1} in China (Wang et al., 2022). These extremes likely reflect significant regional difference in $PM_{2.5}$ sources, as evidenced by the wide CIs in $OP_v^{PM2.5}$ CRF. Such variability highlights the necessity of source-based analyses to accurately assess $PM_{2.5}$-related health effects.

We further evaluated the OP_m of source-specific $PM_{2.5}$ (OP_m^{source}), as detailed in Fig. 2b and Eq. (1). Comparing OP_m^{source} across studies is complicated by inconsistent source categorization; nonetheless, our estimates are within the ranges of prior research (Supplementary Table 11). ENE and TRO sectors demonstrated the highest OP_m^{source} values, at 60 and 49 pmol min^{-1} μg^{-1}, respectively, followed by IND and AGS + RCO. These results corroborate findings from China, where coal combustion exhibited the highest OP_m of 88 pmol min^{-1} μg^{-1} (Liu et al., 2018), as well as reports of elevated OP_m from vehicle emissions in the US (Bates et al., 2015), Europe (Daellenbach et al., 2020), and marine vessels in Hong Kong (Cheng et al., 2021). Conversely, OP_m^{source} for IND and AGS + RCO was 2–4 times lower than for ENE and TRO, aligning with ranges documented for industrial sources (Cesari et al., 2019; Liu et al., 2018) and biomass burning (Cheng et al., 2021; Liu et al., 2018). These differences in OP_m^{source} can be attributed to varying concentrations of key OP drivers, including metals (e.g., Cu, Mn, V, Ni, As) and organic compounds such as oxygenated polycyclic aromatic hydrocarbons (O-PAHs) (Bates et al., 2019). The elevated OP_m^{source} for ENE and TRO likely stems from higher metal content in emissions from coal-fired power plants and vehicles compared to IND and AGS + RCO (Alias et al., 2020; Reff et al., 2009; Wu et al., 2022; Zhao et al., 2021), while PAH concentrations vary across all sources types (Shen et al., 2013; Wu et al., 2022).

The OP_v^{source} distributions derived from our analysis (Fig. 3) corresponded closely with measured $PM_{2.5}$ OP_v values reported across multiple countries (Supplementary Table 12 and Fig. 3 inset). Among nations with the highest estimated exposures, Pakistan recorded an OP_v^{source} of 3.29 ± 1.11 nmol min^{-1} m^{-3}, comparable to 8.9 ± 3.8 nmol min^{-1} m^{-3} measured in February 2019 (Ahmad et al., 2021). Similarly, India (2.50 ± 1.51 nmol min^{-1} m^{-3}) and China (2.38 ± 1.06 nmol min^{-1} m^{-3}) showed estimates consistent with observed values of 2.90 ± 1.10 nmol min^{-1} m^{-3} in Delhi (Verma et al., 2024) and 2.2–2.9 nmol min^{-1} m^{-3} in Nanjing (Zhang et al., 2023a), Beijing (Campbell et al., 2021), and Wuhan (Liu et al., 2020). Statistical analysis revealed strong agreement between our estimates and actual measurements (slope = 1.0011, $R^2 = 0.95$, MAE = 0.24 nmol min^{-1} m^{-3}, RMSE = 0.31 nmol min^{-1} m^{-3}, Fig. 3 inset), affirming the reliability of our OP_v^{source} CRFs. Globally, ENE (39 %) and TRO (33 %) sectors dominate the average OP_v^{source}. This is consistent with prior research linking elevated OP exposure to fossil fuel combustion and vehicular emissions (Bhattu et al., 2024; Campbell et al., 2021; Daellenbach et al., 2020), a pattern supported by the high intrinsic OP_m^{source} of these sectors (Fig. 2b). These robust comparisons across diverse spatial scales indicate that our estimates align with measured data, suggesting that our OP_v^{source} CRFs are globally applicable.

4.2. Global and national OP_v and source sector contributions for 203 countries in 2017

To estimate the global distribution of OP_v from various sources (OP_v^{source}), we employed our OP_v^{source} CRFs alongside national-level source exposure data for 2017. These estimates highlight critical disparities in sectoral contributions to $PM_{2.5}$ mass (McDuffie et al., 2021) and OP_v^{source} across regions (Figs. 4 and 5), emphasizing the inadequacy of $PM_{2.5}$ alone as a metric for health risk mitigation.

As the first study to assess OP_v^{source} on a global scale, quantitative comparisons with earlier research are not possible for all countries. For countries with OP_v data, it is complicated by inconsistencies in source sector categorization, which have typically been tailored to local-scale studies. Nevertheless, we have aligned out findings with the most relevant existing analyses where possible. Globally, ENE and AGS + RCO sectors emerged as the largest contributors to OP_v^{source} in 2017, accounting for 33 % and 31 %, respectively, followed by TRO at 20 % and IND at 16 % (Fig. 4). These trends align broadly with source apportionment data from 50 countries (1990–2022), where ENE (39 %), TRO (33 %), AGS + RCO (19 %), and IND (9 %) prevailed (Fig. 3). Discrepancies between global and regional estimates likely stem from limited source apportionment data for countries with high industrial activity, such as Peru, or from variations in AGS + RCO data for nations like Nigeria, Bangladesh, and Pakistan. Additionally, evolving technologies and policies over time may further influence sector-specific contributions.

Regionally, fossil fuel combustion (coal, oil, natural gas) drove elevated OP_v^{source} contributions from the ENE sector in Southern Sub-Saharan Africa, Eastern Europe, North Africa/Middle East, and Central Asia (Fig. 5c). This dominance reflects the sector's substantial contribution to $PM_{2.5}$ mass, particularly from burning of coal, oil, and natural gas in countries such as Egypt, Russia, Ukraine, and Turkey (McDuffie et al., 2021), combined with the high OP_m of energy-related $PM_{2.5}$. In contrast, biomass burning, including household biofuels (McDuffie et al., 2021) and agricultural residues (Bhattu et al., 2024; McDuffie et al., 2021), amplified AGS + RCO contributions in Central, Western, and Eastern Sub-Saharan Africa and Oceania. Despite AGS + RCO's lower OP_m (Fig. 2b), rising emissions in Europe (Zauli-Sajani et al., 2024) and Asia (Fang et al., 2023; Lan et al., 2022) suggest growing oxidative burdens in these regions. TRO emerged as a key contributor in Western Europe (36.6 % of OP_v^{source}) and North America (33.2 %), where its high OP_m outweighed AGS + RCO's larger $PM_{2.5}$ mass share (40.7 % and 43.7 %, respectively; Fig. 5a) (McDuffie et al., 2021). Similarly, industrial activities dominated OP_v^{source} in Tropical and Andean Latin America, reflecting substantial IND-sector $PM_{2.5}$ emissions in Brazil and Mexico (McDuffie et al., 2021).

These spatial heterogeneities underscore the necessity for region-specific mitigation strategies. In ENE-dominant regions, transitioning to cleaner energy sources (e.g., renewables, natural gas) could substantially reduce oxidative burdens. AGS + RCO hotspots require targeted interventions, such as agricultural residue management and adoption of clean cooking technologies, to offset the health impacts of biomass combustion. In regions where TRO or IND sectors prevail, stricter vehicle emission standards and industrial process controls are critical. Collectively, these findings demonstrate that mitigating $PM_{2.5}$-related oxidative burden demands tailored approaches addressing dominant local sources, rather than relying solely on $PM_{2.5}$ mass reductions.

4.3. Association between estimated OP_v and mortality for 203 countries in 2017

While OP has been linked to health impacts, the relative importance of source-resolved OP (OP_v^{source}) versus total $PM_{2.5}$ OP ($OP_v^{PM2.5}$) in driving mortality remained unclear. Our analysis demonstrated that OP_v^{source} exhibits a stronger correlation with all-cause mortality than $OP_v^{PM2.5}$ (Fig. 6a). Poisson regression model further confirmed this hierarchy: in single-pollutant models, OP_v^{source} showed the highest standardized coefficients (β), followed by $OP_v^{PM2.5}$ and $PM_{2.5}$ mass, which had comparable effects (Fig. 6b). These findings align with prior regional studies associating $OP_v^{PM2.5}$ with morbidity (Abrams et al., 2017; Bates et al., 2015; Fang et al., 2016) and mortality (Atkinson et al., 2016) (Supplementary Table 14), though no global-scale analysis had previously linked $OP_v^{PM2.5}$ or OP_v^{source} to mortality. Notably, in a three-pollutant model accounting for $PM_{2.5}$ mass, $OP_v^{PM2.5}$, and OP_v^{source}, only OP_v^{source} retained statistical significance (Fig. 6b), a pattern consistent with U.S. studies reporting null effects for $PM_{2.5}$ mass in bi-pollutant models assessing emergency department visits (Bates et al., 2015). These results underscore that OP_v^{source}, which was estimated first in this study, may capture $PM_{2.5}$ health risks more robustly than bulk OP or mass metrics.

Sector-specific analyses revealed that all anthropogenic sources contributed significantly to mortality in single-pollutant models (Fig. 6c, Supplementary Fig. 4), mirroring their OP_m rankings (Fig. 2a). However, in multi-source models, only IND and TRO OP_v^{source} remained significant (Fig. 6d). This divergence likely reflects the distinct redox-active components of these sectors: IND emissions are enriched in heavy metals (e.g., Cu, Mn, Fe), while TRO emissions contain organic aerosol, such as O-PAHs (Zhang et al., 2023c)–both known drivers of oxidative stress (Esu et al., 2024).

4.4. Implications for risk and life cycle impact assessment

Our findings carry significant implications for human health risk assessment and life cycle impact assessment (LCIA) frameworks. While these frameworks have evolved beyond simple $PM_{2.5}$ mass metrics—now routinely linking exposure to cause-specific health outcomes such as cardiovascular and respiratory diseases, and expressing impacts in disability-adjusted life years (DALYs) or years of life lost—they still rely fundamentally on $PM_{2.5}$ mass as the exposure proxy. Despite growing toxicological and epidemiological evidence that OP better reflects the biological activity of $PM_{2.5}$ and may serve as a more health-relevant exposure metric, OP remains largely absent from mainstream impact assessment methodologies. This gap stems from three interrelated challenges: (1) OP measurements have historically been sparse, methodologically inconsistent (e.g., DTT vs. ascorbic acid assays), and geographically limited, hindering global application; (2) Until now, there has been no robust, source-resolved, globally applicable model linking emissions to OP; and (3) While evidence linking OP to adverse health outcomes is rapidly accumulating (Qin et al., 2024), it remains less extensive than the decades of research underpinning $PM_{2.5}$ mass–health relationships.

Our study directly addresses the second barrier by providing a harmonized global dataset and a source-specific OP prediction framework. In light of this progress, we recommend that developers of risk and LCIA methods begin integrating oxidative burden—alongside $PM_{2.5}$ mass—as a complementary exposure indicator in human health impact models.

To meaningfully integrate OP into existing impact pathways, we propose a refined, mechanistically grounded framework that improves current mass-based approaches by explicitly accounting for respiratory deposition and biological activity (Fig. 7):

1. Deposited source-specific $PM_{2.5}$ mass quantification: Size-resolved source-specific concentrations (Exposure I) are translated into the fraction of source-specific $PM_{2.5}$ (Exposure II) that is actually inhaled and deposited in the respiratory tract. This can be obtained using established deposition models such as those from the International Commission on Radiological Protection (ICRP) or the Multiple Path Particle Dosimetry (MPPD) model. Traditional LCIA and risk assessments often omit this step, potentially misrepresenting true internal dose.
2. Deposited source-specific OP exposure calculation: The deposited source-specific $PM_{2.5}$ mass (Exposure II) is then converted to OP using our source–OP relationship (Equation (1)). This yields OP as the oxidative burden (nmol/min/m^3), a metric that reflects not just how much PM is inhaled, but how biologically active it is via the oxidative stress pathway.
3. Dose–response modeling: Derive concentration–response functions linking OP_v to cause-specific mortality and morbidity outcomes.
4. Impact quantification: Apply these functions to calculate health impacts attributable to oxidative burden from specific emission sources.

Step 2 is now feasible thanks to the present work. Step 3 remains a critical priority for future epidemiological and modeling research. Encouragingly, progress is already underway: standardized, low-cost OP measurement protocols are being established (Dominutti et al., 2025), which will help address the data limitations that have historically constrained such efforts. Even though OP captures a key mechanism of $PM_{2.5}$ toxicity, namely oxidative stress, PM can also cause harm through other pathways, such as inflammation, metal-induced toxicity, and physical translocation into biological systems. For this reason, OP should complement—not replace—$PM_{2.5}$ mass in health impact assessments, offering a more mechanistically informed dimension of risk without discarding the well-established value of mass-based metrics.

5. Conclusions

This study presents the first global estimation of OP CRFs for $PM_{2.5}$ and its major anthropogenic sources, advancing our capacity to evaluate oxidative burden and its mortality linkages worldwide. Our findings challenge conventional reliance on total $PM_{2.5}$ mass or bulk oxidative potential ($OP_v^{PM2.5}$) as health metrics, demonstrating that source-

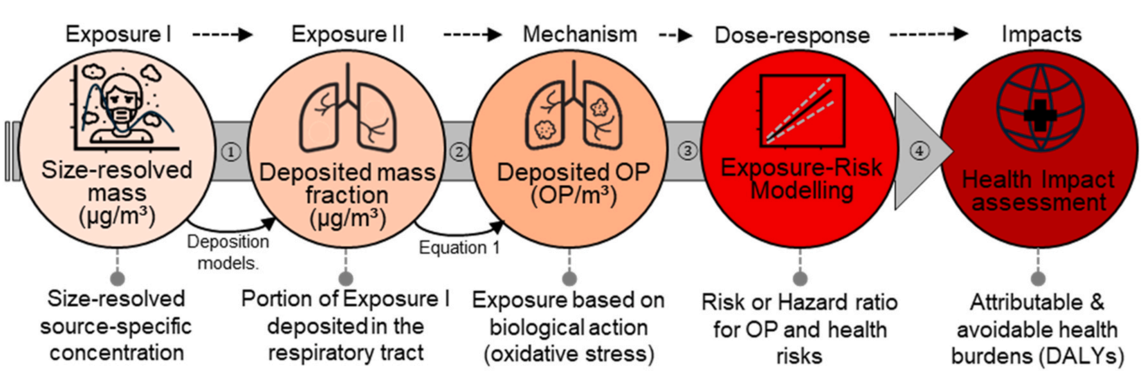

Fig. 7. | Conceptual framework for integrating OP into $PM_{2.5}$ health risk assessment.

resolved oxidative potential (OP_v^{source}) offers superior precision in mortality risk assessment. Specifically, energy (ENE) and transportation (TRO) sectors exhibited the highest intrinsic OP (OP_m), and TRO and industrial (IND) sectors exhibited the strongest mortality associations, while agriculture/residential-commercial (AGS + RCO) emerged as the second-largest contributor to global OP_v^{source} in 2017 due to its high $PM_{2.5}$ concentrations in key regions. Critically, multi-pollutant models identified OP_v^{source} as the sole significant mortality driver, underscoring the limitations of $PM_{2.5}$ mass-based frameworks.

These results necessitate a paradigm shift in air quality management. Policymakers should prioritize emissions controls tailored to dominant local sources of oxidative burden:

1. ENE/TRO-Dominant Regions (e.g., Eastern Europe, North America): Target fossil fuel combustion (coal, oil) and vehicular emissions through cleaner energy transitions and stricter vehicle standards.
2. AGS + RCO Hotspots (e.g., Sub-Saharan Africa, Oceania): Implement agricultural residue management and clean cooking technologies to mitigate biomass burning impacts.
3. IND-Intensive Areas (e.g., Latin America): Strengthen industrial process controls to reduce metal-rich particulate emissions.

The spatial heterogeneity of OP_v^{source} contributions underscores the inefficiency of one-size-fits-all strategies. Localized interventions, informed by source-specific CRFs, will optimize resource allocation and health outcomes. Future research should prioritize the expansion of global OP_v^{source} monitoring networks to include more refined source categories, particularly those that capture secondary formation processes (e.g., oxidative transformation of PAHs) (Esu and Cho, 2025). Additionally, studies should investigate causal links between source-specific OP_v and cause-specific mortality and morbidity, with a focus on underrepresented regions. Such efforts will help pinpoint the specific anthropogenic activities and atmospheric processes that drive oxidative potential exposure at local scales. By elucidating the contribution of anthropogenic sources in $PM_{2.5}$ toxicity, this work provides a foundation for precision air quality policies that address both particulate mass and oxidative health risks.

CRediT authorship contribution statement

Charles O. Esu: Writing – original draft, Formal analysis, Conceptualization. **Kuk Cho:** Writing – review & editing, Validation, Conceptualization.

Funding

This study was supported by the National Research Foundation (NRF) grants funded by the Ministry of Education, Republic of Korea [Grant No. RS-2020-NR049592].

Declaration of competing interest

The authors declare the following financial interests/personal relationships which may be considered as potential competing interests: Kuk Cho reports financial support was provided by National Research Foundation of Korea. If there are other authors, they declare that they have no known competing financial interests or personal relationships that could have appeared to influence the work reported in this paper.

Appendix A. Supplementary data

Supplementary data to this article can be found online at https://doi.org/10.1016/j.jenvman.2025.127920.

Data availability

Data will be made available on request.

References

Abrams, J.Y., Weber, R.J., Klein, M., Samat, S.E., Chang, H.H., Strickland, M.J., Verma, V., Fang, T., Bates, J.T., Mulholland, J.A., Russell, A.G., Tolbert, P.E., 2017. Associations between ambient fine particulate oxidative potential and cardiorespiratory emergency department visits. Environ. Health Perspect. 125, 107008. https://doi.org/10.1289/ehp1545.

Ahmad, M., Yu, Q., Chen, J., Cheng, S., Qin, W., Zhang, Y., 2021. Chemical characteristics, oxidative potential, and sources of $PM_{2.5}$ in wintertime in Lahore and Peshawar, Pakistan. J. Environ. Sci. 102, 148–158. https://doi.org/10.1016/j.jes.2020.09.014.

Aldekheel, M., Tohidi, R., Al-Hemoud, A., Alkudari, F., Verma, V., Subramanian, P.S.G., Sioutas, C., 2024. Identifying urban emission sources and their contribution to the oxidative potential of fine particulate matter (PM2.5) in Kuwait. Environ. Pollut. 343, 123165. https://doi.org/10.1016/j.envpol.2023.123165.

Alias, N.F., Khan, M.F., Sairi, N.A., Zain, S.M., Suradi, H., Rahim, H.A., Banerjee, T., Bari, M.A., Othman, M., Latif, M.T., 2020. Characteristics, emission sources, and risk factors of heavy metals in $PM_{2.5}$ from Southern Malaysia. ACS Earth Space Chem. 4, 1309–1323. https://doi.org/10.1021/acsearthspacechem.0c00103.

Atkinson, R.W., Samoli, E., Analitis, A., Fuller, G.W., Green, D.C., Anderson, H.R., Purdie, E., Dunster, C., Aitlhadj, L., Kelly, F.J., Mudway, I.S., 2016. Short-term associations between particle oxidative potential and daily mortality and hospital admissions in London. Int. J. Hyg Environ. Health 219, 566–572. https://doi.org/10.1016/j.ijheh.2016.06.004.

Bates, J.T., Fang, T., Verma, V., Zeng, L., Weber, R.J., Tolbert, P.E., Abrams, J.Y., Sarnat, S.E., Klein, M., Mulholland, J.A., Russell, A.G., 2019. Review of acellular assays of ambient particulate matter oxidative potential: methods and relationships with composition, sources, and health effects. Environ. Sci. Technol. 53, 4003–4019. https://doi.org/10.1021/acs.est.8b03430.

Bates, J.T., Weber, R.J., Abrams, J., Verma, V., Fang, T., Klein, M., Strickland, M.J., Sarnat, S.E., Chang, H.H., Mulholland, J.A., Tolbert, P.E., Russell, A.G., 2015. Reactive oxygen species generation linked to sources of atmospheric particulate matter and cardiorespiratory effects. Environ. Sci. Technol. 49, 13605–13612. https://doi.org/10.1021/acs.est.5b02967.

Bhattu, D., Tripathi, S.N., Bhowmik, H.S., Moschos, V., Lee, C.P., Rauber, M., Salazar, G., Abbaszade, G., Cui, T., Slowik, J.G., Vats, P., Mishra, S., Lalchandani, V., Satish, R., Rai, P., Casotto, R., Tobler, A., Kumar, V., Hao, Y., Qi, L., Khare, P., Manousakas, M. I., Wang, Q., Han, Y., Tian, J., Darfeuil, S., Minguillon, M.C., Hueglin, C., Conil, S., Rastogi, N., Srivastava, A.K., Ganguly, D., Bjelic, S., Canonaco, F., Schnelle-Kreis, J., Dominutti, P.A., Jaffrezo, J.-L., Szidat, S., Chen, Y., Cao, J., Baltensperger, U., Uzu, G., Daellenbach, K.R., El Haddad, I., Prévôt, A.S.H., 2024. Local incomplete combustion emissions define the $PM_{2.5}$ oxidative potential in Northern India. Nat. Commun. 15, 3517. https://doi.org/10.1038/s41467-024-47785-5.

Burnett, R., Chen, H., Szyszkowicz, M., Fann, N., Hubbell, B., Pope, C.A., Apte, J.S., Brauer, M., Cohen, A., Weichenthal, S., Coggins, J., Di, Q., Brunekreef, B., Frostad, J., Lim, S.S., Kan, H., Walker, K.D., Thurston, G.D., Hayes, R.B., Lim, C.C., Turner, M.C., Jerrett, M., Krewski, D., Gapstur, S.M., Diver, W.R., Ostro, B., Goldberg, D., Crouse, D.L., Martin, R.V., Peters, P., Pinault, L., Tjepkema, M., van Donkelaar, A., Villeneuve, P.J., Miller, A.B., Yin, P., Zhou, M., Wang, L., Janssen, N. A.H., Marra, M., Atkinson, R.W., Tsang, H., Quoc Thach, T., Cannon, J.B., Allen, R. T., Hart, J.E., Laden, F., Cesaroni, G., Forastiere, F., Weinmayr, G., Jaensch, A., Nagel, G., Concin, H., Spadaro, J.V., 2018. Global estimates of mortality associated with long-term exposure to outdoor fine particulate matter. Proc. Natl. Acad. Sci. 115, 9592–9597. https://doi.org/10.1073/pnas.1803222115.

Burnett, R.T., Pope, C.A., Ezzati, M., Olives, C., Lim, S.S., Mehta, S., Shin, H.H., Singh, G., Hubbell, B., Brauer, M., Anderson, H.R., Smith, K.R., Balmes, J.R., Bruce, N.G., Kan, H., Laden, F., Prüss-Ustün, A., Turner, M.C., Gapstur, S.M., Diver, W.R., Cohen, A., 2014. An integrated risk function for estimating the global burden of disease attributable to ambient fine particulate matter exposure. Environ. Health Perspect. 122, 397–403. https://doi.org/10.1289/ehp.1307049.

Campbell, S.J., Wolfer, K., Utinger, B., Westwood, J., Zhang, Z.H., Bukowiecki, N., Steimer, S.S., Vu, T.V., Xu, J., Straw, N., Thomson, S., Elzein, A., Sun, Y., Liu, D., Li, L., Fu, P., Lewis, A.C., Harrison, R.M., Bloss, W.J., Loh, M., Miller, M.R., Shi, Z., Kalberer, M., 2021. Atmospheric conditions and composition that influence $PM_{2.5}$ oxidative potential in Beijing, China. Atmos. Chem. Phys. 21, 5549–5573. https://doi.org/10.5194/acp-21-5549-2021.

Cesari, D., Merico, E., Grasso, F.M., Decesari, S., Belosi, F., Manarini, F., De Nuntiis, P., Rinaldi, M., Volpi, F., Gambaro, A., Morabito, E., Contini, D., 2019. Source apportionment of $PM_{2.5}$ and of its oxidative potential in an industrial suburban site in South Italy. Atmosphere.

Cheng, Y., Ma, Y., Dong, B., Qiu, X., Hu, D., 2021. Pollutants from primary sources dominate the oxidative potential of water-soluble $PM_{2.5}$ in Hong Kong in terms of dithiothreitol (DTT) consumption and hydroxyl radical production. J. Hazard Mater. 405, 124218. https://doi.org/10.1016/j.jhazmat.2020.124218.

Crobeddu, B., Aragao-Santiago, L., Bui, L.-C., Boland, S., Baeza Squiban, A., 2017. Oxidative potential of particulate matter 2.5 as predictive indicator of cellular stress. Environ. Pollut. 230, 125–133. https://doi.org/10.1016/j.envpol.2017.06.051.

Daellenbach, K.R., Uzu, G., Jiang, J., Cassagnes, L.-E., Leni, Z., Vlachou, A., Stefenelli, G., Canonaco, F., Weber, S., Segers, A., Kuenen, J.J.P., Schaap, M., Favez, O., Albinet, A., Aksoyoglu, S., Dommen, J., Baltensperger, U., Geiser, M., El Haddad, I., Jaffrezo, J.-L., Prévôt, A.S.H., 2020. Sources of particulate-matter air pollution and its oxidative potential in Europe. Nature 587, 414–419. https://doi.org/10.1038/s41586-020-2902-8.

Deng, M., Chen, D., Zhang, G., Cheng, H., 2022. Policy-driven variations in oxidation potential and source apportionment of $PM_{2.5}$ in Wuhan, central China. Sci. Total Environ. 853, 158255. https://doi.org/10.1016/j.scitotenv.2022.158255.

Dominutti, P.A., Jaffrezo, J.L., Marsal, A., Mhadhbi, T., Elazzouzi, R., Rak, C., Cavalli, F., Putaud, J.P., Bougiatioti, A., Mihalopoulos, N., Paraskevopoulou, D., Mudway, I., Nenes, A., Daellenbach, K.R., Banach, C., Campbell, S.J., Cigánková, H., Contini, D., Evans, G., Georgopoulou, M., Ghanem, M., Glencross, D.A., Guascito, M.R., Herrmann, H., Iram, S., Jovanović, M., Jovašević-Stojanović, M., Kalberer, M., Kooter, I.M., Paulson, S.E., Patel, A., Perdrix, E., Pietrogrande, M.C., Mikuška, P., Sauvain, J.J., Seitanidi, K., Shahpoury, P., Souza, E.J.d.S., Steimer, S., Stevanovic, S., Suarez, G., Subramanian, P.S.G., Utinger, B., van Os, M.F., Verma, V., Wang, X., Weber, R.J., Yang, Y., Querol, X., Hoek, G., Harrison, R.M., Uzu, G., 2025. An interlaboratory comparison to quantify oxidative potential measurement in aerosol particles: challenges and recommendations for harmonisation. Atmos. Meas. Tech. 18, 177–195. https://doi.org/10.5194/amt-18-177-2025.

Esu, C.O., Cho, K., 2025. Explainable machine learning reveals the potential contribution of metals to PAH degradation in particulate matter. J. Environ. Chem. Eng. 13, 117769. https://doi.org/10.1016/j.jece.2025.117769.

Esu, C.O., Pyo, J., Cho, K., 2024. Machine learning-derived dose-response relationships considering interactions in mixtures: applications to the oxidative potential of particulate matter. J. Hazard Mater. 475, 134864. https://doi.org/10.1016/j.jhazmat.2024.134864.

Fang, T., Verma, V., Bates, J.T., Abrams, J., Klein, M., Strickland, M.J., Sarnat, S.E., Chang, H.H., Mulholland, J.A., Tolbert, P.E., Russell, A.G., Weber, R.J., 2016. Oxidative potential of ambient water-soluble $PM_{2.5}$ in the southeastern United States: contrasts in sources and health associations between ascorbic acid (AA) and dithiothreitol (DTT) assays. Atmos. Chem. Phys. 16, 3865–3879. https://doi.org/10.5194/acp-16-3865-2016.

Fang, W., Evangeliou, N., Eckhardt, S., Xing, J., Zhang, H., Xiao, H., Zhao, M., Kim, S.-W., 2023. Increased contribution of biomass burning to haze events in Shanghai since China's clean air actions. Commun. Earth Environ. 4, 310. https://doi.org/10.1038/s43247-023-00979-z.

Giannossa, L.C., Cesari, D., Merico, E., Dinoi, A., Mangone, A., Guascito, M.R., Contini, D., 2022. Inter-annual variability of source contributions to PM10, PM2.5, and oxidative potential in an urban background site in the central mediterranean. J. Environ. Manag. 319, 115752. https://doi.org/10.1016/j.jenvman.2022.115752.

He, L., Norris, C., Cui, X., Li, Z., Barkjohn, K.K., Brehmer, C., Teng, Y., Fang, L., Lin, L., Wang, Q., Zhou, X., Hong, J., Li, F., Zhang, Y., Schauer, J.J., Black, M., Bergin, M.H., Zhang, J.J., 2021. Personal exposure to $PM_{2.5}$ oxidative potential in Association with pulmonary pathophysiologic outcomes in children with asthma. Environ. Sci. Technol. 55, 3101–3111. https://doi.org/10.1021/acs.est.0c06114.

Hopke, P.K., Dai, Q., Li, L., Feng, Y., 2020. Global review of recent source apportionments for airborne particulate matter. Sci. Total Environ. 740, 140091. https://doi.org/10.1016/j.scitotenv.2020.140091.

Janssen, N.A.H., Strak, M., Yang, A., Hellack, B., Kelly, F.J., Kuhlbusch, T.A.J., Harrison, R.M., Brunekreef, B., Cassee, F.R., Steenhof, M., Hoek, G., 2015. Associations between three specific a-cellular measures of the oxidative potential of particulate matter and markers of acute airway and nasal inflammation in healthy volunteers. Occup. Environ. Med. 72, 49–56. https://doi.org/10.1136/oemed-2014-102303.

Kim, P.-R., Park, S.-W., Han, Y.-J., Lee, M.-H., Holsen, T.M., Jeong, C.-H., Evans, G., 2024. Variations of oxidative potential of $PM_{2.5}$ in a medium-sized residential city in South Korea measured using three different chemical assays. Sci. Total Environ. 920, 171053. https://doi.org/10.1016/j.scitotenv.2024.171053.

Kurihara, K., Iwata, A., Murray Horwitz, S.G., Ogane, K., Sugioka, T., Matsuki, A., Okuda, T., 2022. Contribution of physical and chemical properties to dithiothreitol-measured oxidative potentials of atmospheric aerosol particles at urban and rural sites in Japan. Atmosphere 13, 319.

Lakey, P.S.J., Berkemeier, T., Tong, H., Arangio, A.M., Lucas, K., Pöschl, U., Shiraiwa, M., 2016. Chemical exposure-response relationship between air pollutants and reactive oxygen species in the human respiratory tract. Sci. Rep. 6, 32916. https://doi.org/10.1038/srep32916.

Lan, R., Eastham, S.D., Liu, T., Norford, L.K., Barrett, S.R.H., 2022. Air quality impacts of crop residue burning in India and mitigation alternatives. Nat. Commun. 13, 6537. https://doi.org/10.1038/s41467-022-34093-z.

Lavigne, É., Burnett, R.T., Stieb, D.M., Evans, G.J., Pollitt, K.J.G., Chen, H., Rijswijk, D.v., Weichenthal, S., 2018. Fine particulate air pollution and adverse birth outcomes: effect modification by regional nonvolatile oxidative potential. Environ. Health Perspect. 126, 077012. https://doi.org/10.1289/EHP2535.

Lelieveld, J., Evans, J.S., Fnais, M., Giannadaki, D., Pozzer, A., 2015. The contribution of outdoor air pollution sources to premature mortality on a global scale. Nature 525, 367–371. https://doi.org/10.1038/nature15371.

Li, C., Hakkim, H., Sinha, V., Sinha, B., Pardo, M., Cai, D., Reicher, N., Chen, J., Hao, K., Rudich, Y., 2024. Variation of $PM_{2.5}$ redox potential and toxicity during monsoon in Delhi, India. ACS ES&T Air 1, 316–329. https://doi.org/10.1021/acsestair.3c00096.

Liu, C., Chen, R., Sera, F., Vicedo-Cabrera, A.M., Guo, Y., Tong, S., Coelho, M.S.Z.S., Saldiva, P.H.N., Lavigne, E., Matus, P., Valdes Ortega, N., Osorio Garcia, S., Pascal, M., Stafoggia, M., Scortichini, M., Hashizume, M., Honda, Y., Hurtado-Díaz, M., Cruz, J., Nunes, B., Teixeira, J.P., Kim, H., Tobias, A., Íñiguez, C., Forsberg, B., Åström, C., Ragettli, M.S., Guo, Y.-L., Chen, B.-Y., Bell, M.L., Wright, C. Y., Scovronick, N., Garland, R.M., Milojevic, A., Kyselý, J., Urban, A., Orru, H., Indermitte, E., Jaakkola, J.J.K., Ryti, N.R.I., Katsouyanni, K., Analitis, A., Zanobetti, A., Schwartz, J., Chen, J., Wu, T., Cohen, A., Gasparrini, A., Kan, H., 2019. Ambient particulate air pollution and daily mortality in 652 cities. N. Engl. J. Med. 381, 705–715. https://doi.org/10.1056/NEJMoa1817364.

Liu, Q., Baumgartner, J., Zhang, Y., Liu, Y., Sun, Y., Zhang, M., 2014. Oxidative potential and inflammatory impacts of source apportioned ambient air pollution in Beijing. Environ. Sci. Technol. 48, 12920–12929. https://doi.org/10.1021/es5029876.

Liu, Q., Lu, Z., Xiong, Y., Huang, F., Zhou, J., Schauer, J.J., 2020. Oxidative potential of ambient $PM_{2.5}$ in Wuhan and its comparisons with eight areas of China. Sci. Total Environ. 701, 134844. https://doi.org/10.1016/j.scitotenv.2019.134844.

Liu, W., Xu, Y., Liu, W., Liu, Q., Yu, S., Liu, Y., Wang, X., Tao, S., 2018. Oxidative potential of ambient $PM_{2.5}$ in the coastal cities of the Bohai Sea, northern China: seasonal variation and source apportionment. Environ. Pollut. 236, 514–528. https://doi.org/10.1016/j.envpol.2018.01.116.

McDuffie, E.E., Martin, R.V., Spadaro, J.V., Burnett, R., Smith, S.J., O'Rourke, P., Hammer, M.S., van Donkelaar, A., Bindle, L., Shah, V., Jaeglé, L., Luo, G., Yu, F., Adeniran, J.A., Lin, J., Brauer, M., 2021. Source sector and fuel contributions to ambient $PM_{2.5}$ and attributable mortality across multiple spatial scales. Nat. Commun. 12, 3594. https://doi.org/10.1038/s41467-021-23853-y.

Murray, C.J.L., Aravkin, A.Y., Zheng, P., Abbafati, C., Abbas, K.M., Abbasi-Kangevari, M., Abd-Allah, F., Abdelalim, A., Abdollahi, M., Abdollahpour, I., Abegaz, K.H., Abolhassani, H., Aboyans, V., Abreu, L.G., Abrigo, M.R.M., Abualhasan, A., Abu-Raddad, L.J., Abushouk, A.I., Adabi, M., Adekanmbi, V., Adeoye, A.M., Adetokunboh, O.O., Adham, D., Advani, S.M., Agarwal, G., Aghamir, S.M.K., Agrawal, A., Ahmad, T., Ahmadi, K., Ahmadi, M., Ahmadieh, H., Ahmed, M.B., Akalu, T.Y., Akinyemi, R.O., Akinyemiju, T., Akombi, B., Akunna, C.J., Alahdab, F., Al-Aly, Z., Alam, K., Alam, S., Alam, T., Alanezi, F.M., Alanzi, T.M., Alemu, B.w., Alhabib, K.F., Ali, M., Ali, S., Alicandro, G., Alinia, C., Alipour, V., Alizade, H., Aljunid, S.M., Alla, F., Allebeck, P., Almasi-Hashiani, A., Al-Mekhlafi, H.M., Alonso, J., Altirkawi, K.A., Amini-Rarani, M., Amiri, F., Amugsi, D.A., Ancuceanu, R., Anderlini, D., Anderson, J.A., Andrei, C.L., Andrei, T., Angus, C., Anjomshoa, M., Ansari, F., Ansari-Moghaddam, A., Antonazzo, I.C., Antonio, C.A.T., Antony, C.M., Antriyandarti, E., Anvari, D., Anwer, R., Appiah, S.C.Y., Arabloo, J., Arab-Zozani, M., Ariani, F., Armoon, B., Ärnlöv, J., Arzani, A., Asadi-Aliabadi, M., Asadi-Pooya, A.A., Ashbaugh, C., Assmus, M., Atafar, Z., Atnafu, D.D., Atout, M.M.d. W., Ausloos, F., Ausloos, M., Ayala Quintanilla, B.P., Ayano, G., Ayanore, M.A., Azari, S., Azarian, G., Azene, Z.N., Badawi, A., Badiye, A.D., Bahrami, M.A., Bakhshaei, M.H., Bakhtiari, A., Bakkannavar, S.M., Baldasseroni, A., Ball, K., Ballew, S.H., Balzi, D., Banach, M., Banerjee, S.K., Bante, A.B., Baraki, A.G., Barker-Collo, S.L., Bärnighausen, T.W., Barrero, L.H., Barthelemy, C.M., Barua, L., Basu, S., Baune, B.T., Bayati, M., Becker, J.S., Bedi, N., Beghi, E., Béjot, Y., Bell, M.L., Bennitt, F.B., Bensenor, I.M., Berhe, K., Berman, A.E., Bhagavathula, A.S., Bhageerathy, R., Bhala, N., Bhandari, D., Bhattacharyya, K., Bhutta, Z.A., Bijani, A., Bikbov, B., Bin Sayeed, M.S., Biondi, A., Birihane, B.M., Bisignano, C., Biswas, R.K., Bitew, H., Bohlouli, S., Bohluli, M., Boon-Dooley, A.S., Borges, G., Borzì, A.M., Borzouei, S., Bosetti, C., Boufous, S., Braithwaite, D., Breitborde, N.J.K., Breitner, S., Brenner, H., Briant, P.S., Briko, A.N., Briko, N.I., Britton, G.B., Bryazka, D., Bumgarner, B.R., Burkart, K., Burnett, R.T., Burugina Nagaraja, S., Butt, Z.A., Caetano dos Santos, F.L., Cahill, L.E., Cámera, L.L.A.A., Campos-Nonato, I.R., Cárdenas, R., Carreras, G., Carrero, J.J., Carvalho, F., Castaldelli-Maia, J.M., Castañeda-Orjuela, C.A., Castelpietra, G., Castro, F., Causey, K., Cederroth, C.R., Cercy, K.M., Cerin, E., Chandan, J.S., Chang, K.-L., Charlson, F.J., Chattu, V.K., Chaturvedi, S., Cherbuin, N., Chimed-Ochir, O., Cho, D.Y., Choi, J.-Y.J., Christensen, H., Chu, D.-T., Chung, M.T., Chung, S.-C., Cicuttini, F.M., Ciobanu, L.G., Cirillo, M., Classen, T.K.D., Cohen, A.J., Compton, K., Cooper, O.R., Costa, V.M., Cousin, E., Cowden, R.G., Cross, D.H., Cruz, J.A., Dahlawi, S.M.A., Damasceno, A.A. M., Damiani, G., Dandona, L., Dandona, R., Dangel, W.J., Danielsson, A.-K., Dargan, P.I., Darwesh, A.M., Daryani, A., Das, J.K., Das Gupta, R., das Neves, J., Dávila-Cervantes, C.A., Davitoiu, D.V., De Leo, D., Degenhardt, L., DeLang, M., Dellavalle, R.P., Demeke, F.M., Demoz, G.T., Demsie, D.G., Denova-Gutiérrez, E., Dervenis, N., Dhungana, G.P., Dianatinasab, M., Dias da Silva, D., Diaz, D., Dibaji Forooshani, Z.S., Djalalinia, S., Do, H.T., Dokova, K., Dorostkar, F., Doshmangir, L., Driscoll, T.R., Duncan, B.B., Duraes, A.R., Eagan, A.W., Edvardsson, D., El Nahas, N., El Sayed, I., El Tantawi, M., Elbarazi, I., Elgendy, I.Y., El-Jaafary, S.I., Elyazar, I.R.F., Emmons-Bell, S., Erskine, H.E., Eskandarieh, S., Esmaeilnejad, S., Esteghamati, A., Estep, K., Etemadi, A., Etisso, A.E., Fanzo, J., Farahmand, M., Fareed, M., Faridnia, R., Farioli, A., Faro, A., Faruque, M., Farzadfar, F., Fattahi, N., Fazlzadeh, M., Feigin, V.L., Feldman, R., Fereshtehnejad, S.-M., Fernandes, E., Ferrara, G., Ferrari, A.J., Ferreira, M.L., Filip, I., Fischer, F., Fisher, J.L., Flor, L.S., Foigt, N.A., Folayan, M.O., Fomenkov, A.A., Force, L.M., Foroutan, M., Franklin, R. C., Freitas, M., Fu, W., Fukumoto, T., Furtado, J.M., Gad, M.M., Gakidou, E., Gallus, S., Garcia-Basteiro, A.L., Gardner, W.M., Geberemariyam, B.S., Gebreslassie, A.A.A.A., Geremew, A., Gershberg Hayoon, A., Gething, P.W., Ghadimi, M., Ghadiri, K., Ghaffarifar, F., Ghafourifard, M., Ghamari, F., Ghashghaee, A., Ghiasvand, H., Ghith, N., Gholamian, A., Ghosh, R., Gill, P.S., Ginindza, T.G.G., Giussani, G., Gnedovskaya, E.V., Goharinezhad, S., Gopalani, S.V., Gorini, G., Goudarzi, H., Goulart, A.C., Greaves, F., Grivna, M., Grosso, G., Gubari, M.I.M., Gugnani, H.C., Guimarães, R.A., Guled, R.A., Guo, G., Guo, Y., Gupta, R., Gupta, T., Haddock, B., Hafezi-Nejad, N., Hafiz, A., Haj-Mirzaian, A., Haj-Mirzaian, A., Hall, B.J., Halvaei, I., Hamadeh, R.R., Hamidi, S., Hammer, M.S., Hankey, G.J., Haririan, H., Haro, J.M., Hasaballah, A.I., Hasan, M.M., Hasanpoor, E., Hashi, A., Hassanipour, S., Hassankhani, H., Havmoeller, R.J., Hay, S.I., Hayat, K., Heidari, G., Heidari-Soureshjani, R., Henrikson, H.J., Herbert, M.E., Herteliu, C., Heydarpour, F., Hird, T.R., Hoek, H.W., Holla, R., Hoogar, P., Hosgood, H.D., Hossain, N., Hosseini, M., Hosseinzadeh, M., Hostiuc, M., Hostiuc, S., Househ, M., Hsairi, M., Hsieh, V.C.-r., Hu, G., Hu, K., Huda, T.M., Humayun, A., Huynh, C.K., Hwang, B.-F., Iannucci, V.C., Ibitoye, S.E., Ikeda, N., Ikuta, K.S., Ilesanmi, O.S., Ilic, I.M., Ilic, M.D., Inbaraj, L.R., Ippolito, H., Iqbal, U., Irvani, S.S.N., Irvine, C.M.S., Islam, M.M., Islam, S.M.S., Iso, H., Ivers, R.Q., Iwu, C.C.D., Iwu, C.J., Iyamu, I.O., Jaafari, J., Jacobsen, K.H., Jafari, H., Jafarinia, M., Jahani, M.A., Jakovljevic, M., Jalilian, F., James, S.L., Janjani, H., Javaheri, T., Javidnia, J., Jeemon, P., Jenabi, E., Jha, R.P., Jha, V., Ji, J.S., Johansson, L., John, O., John-Akinola, Y.O., Johnson, C.O., Jonas, J.B., Joukar, F., Jozwiak, J.J., Jürisson, M., Kabir, A., Kabir, Z., Kalani, H., Kalani, R., Kalankesh, L.R., Kalhor, R., Kanchan, T., Kapoor, N., Karami Matin, B., Karch, A., Karim, M.A., Kassa, G.M., Katikireddi, S.V., Kayode, G.A., Kazemi Karyani, A., Keiyoro, P.N., Keller, C., Kemmer, L., Kendrick, P.J., Khalid, N., Khammarnia, M., Khan, E.A., Khan, M., Khatab, K., Khater, M.M., Khatib, M.N., Khayamzadeh, M., Khazaei, S., Kieling, C., Kim, Y.J., Kimokoti, R.W., Kisa, A., Kisa, S., Kivimäki, M., Knibbs, L.D., Knudsen, A.K.S., Kocarnik, J.M., Kochhar, S., Kopec, J.A., Korshunov, V.A., Koul, P.A., Koyanagi, A., Kraemer, M.U.G., Krishan, K., Krohn, K.J., Kromhout, H., Kuate Defo, B., Kumar, G.A., Kumar, V., Kurmi, O.P., Kusuma, D., La Vecchia, C., Lacey, B., Lal, D.K., Lalloo, R., Lallukka, T., Lami, F.H., Landires, I., Lang, J.J., Langan, S.M., Larsson, A.O., Lasrado, S., Lauriola, P., Lazarus, J.V., Lee, P.H., Lee, S.W.H., LeGrand, K.E., Leigh, J., Leonardi, M., Lescinsky, H., Leung, J., Levi, M., Li, S., Lim, L.-L., Linn, S., Liu, S., Liu, S., Liu, Y., Lo, J., Lopez, A.D., Lopez, J.C.F., Lopukhov, P.D., Lorkowski, S., Lotufo, P.A., Lu, A., Lugo, A., Maddison, E.R., Mahasha, P.W., Mahdavi, M.M., Mahmoudi, M., Majeed, A., Maleki, A., Maleki, S., Malekzadeh, R., Malta, D.C., Mamun, A.A., Manda, A.L., Manguerra, H., Mansour-Ghanaei, F., Mansouri, B., Mansournia, M.A., Mantilla Herrera, A.M., Maravilla, J.C., Marks, A., Martin, R.V., Martini, S., Martins-Melo, F.R., Masaka, A., Masoumi, S.Z., Mathur, M.R., Matsushita, K., Maulik, P.K., McAlinden, C., McGrath, J.J., McKee, M., Mehndiratta, M.M., Mehri, F., Mehta, K. M., Memish, Z.A., Mendoza, W., Menezes, R.G., Mengesha, E.W., Mereke, A., Mereta, S.T., Meretoja, A., Meretoja, T.J., Mestrovic, T., Miazgowski, B., Miazgowski, T., Michalek, I.M., Miller, T.R., Mills, E.J., Mini, G.K., Miri, M., Mirica, A., Mirrakhimov, E.M., Mirzaei, H., Mirzaei, M., Mirzaei, R., Mirzaei-Alavijeh, M., Misganaw, A.T., Mithra, P., Moazen, B., Mohammad, D.K., Mohammad, Y., Mohammad Gholi Mezerji, N., Mohammadian-Hafshejani, A., Mohammadifard, N., Mohammadpourhodki, R., Mohammed, A.S., Mohammed, H., Mohammed, J.A., Mohammed, S., Mokdad, A.H., Molokhia, M., Monasta, L., Mooney, M.D., Moradi, G., Moradi, M., Moradi-Lakeh, M., Moradzadeh, R., Moraga, P., Morawska, L., Morgado-da-Costa, J., Morrison, S.D., Mosapour, A., Mosser, J.F., Mouodi, S., Mousavi, S.M., Mousavi Khaneghah, A., Mueller, U.O., Mukhopadhyay, S., Mullany, E.C., Musa, K.I., Muthupandian, S., Nabhan, A.F., Naderi, M., Nagarajan, A.J., Nagel, G., Naghavi, M., Naghshtabrizi, B., Naimzada, M. D., Najafi, F., Nangia, V., Nansseu, J.R., Naserbakht, M., Nayak, V.C., Negoi, I., Ngunjiri, J.W., Nguyen, C.T., Nguyen, H.L.T., Nguyen, M., Nigatu, Y.T., Nikbakhsh, R., Nixon, M.R., Nnaji, C.A., Nomura, S., Norrving, B., Noubiap, J.J., Nowak, C., Nunez-Samudio, V., Oţoiu, A., Oancea, B., Odell, C.M., Ogbo, F.A., Oh, I.-H., Okunga, E.W., Oladnabi, M., Olagunju, A.T., Olusanya, B.O., Olusanya, J.O., Omer, M.O., Ong, K.L., Onwujekwe, O.E., Orpana, H.M., Ortiz, A., Osarenotor, O., Osei, F.B., Ostroff, S.M., Otstavnov, N., Otstavnov, S.S., Øverland, S., Owolabi, M.O., P A, M., Padubidri, J.R., Palladino, R., Panda-Jonas, S., Pandey, A., Parry, C.D.H., Pasovic, M., Pasupula, D.K., Patel, S.K., Pathak, M., Patten, S.B., Patton, G.C., Pazoki Toroudi, H., Peden, A.E., Pennini, A., Pepito, V.C.F., Peprah, E.K., Pereira, D.M., Pesudovs, K., Pham, H.Q., Phillips, M.R., Piccinelli, C., Pilz, T.M., Piradov, M.A., Pirsaheb, M., Plass, D., Polinder, S., Polkinghorne, K.R., Pond, C.D., Postma, M.J., Pourjafar, H., Pourmalek, F., Poznańska, A., Prada, S.I., Prakash, V., Pribadi, D.R.A., Pupillo, E., Quazi Syed, Z., Rabiee, M., Rabiee, N., Radfar, A., Rafiee, A., Raggi, A., Rahman, M.A., Rajabpour-Sanati, A., Rajati, F., Rakovac, I., Ram, P., Ramezanzadeh, K., Ranabhat, C.L., Rao, P.C., Rao, S.J., Rashedi, V., Rathi, P., Rawaf, D.L., Rawaf, S., Rawal, L., Rawassizadeh, R., Rawat, R., Razo, C., Redford, S. B., Reiner Jr., R.C., Reitsma, M.B., Remuzzi, G., Renjith, V., Renzaho, A.M.N., Resnikoff, S., Rezaei, N., Rezaei, N., Rezapour, A., Rhinehart, P.-A., Riahi, S.M., Ribeiro, D.C., Ribeiro, D., Rickard, J., Rivera, J.A., Roberts, N.L.S., Rodríguez-Ramírez, S., Roever, L., Ronfani, L., Room, R., Roshandel, G., Roth, G.A., Rothenbacher, D., Rubagotti, E., Rwegerera, G.M., Sabour, S., Sachdev, P.S., Saddik, B., Sadeghi, E., Sadeghi, M., Saeedi, R., Saeedi Moghaddam, S., Safari, Y., Safi, S., Safiri, S., Sagar, R., Sahebkar, A., Sajadi, S.M., Salam, N., Salamati, P., Salem, H., Salem, M.R.R., Salimzadeh, H., Salman, O.M., Salomon, J.A., Samad, Z., Samadi Kafil, H., Sambala, E.Z., Samy, A.M., Sanabria, J., Sánchez-Pimienta, T.G., Santomauro, D.F., Santos, I.S., Santos, J.V., Santric-Milicevic, M.M., Saraswathy, S.Y. I., Sarmiento-Suárez, R., Sarrafzadegan, N., Sartorius, B., Sarveazad, A., Sathian, B., Sathish, T., Sattin, D., Saxena, S., Schaeffer, L.E., Schiavolin, S., Schlaich, M.P., Schmidt, M.I., Schutte, A.E., Schwebel, D.C., Schwendicke, F., Senbeta, A.M., Senthilkumaran, S., Sepanlou, S.G., Serdar, B., Serre, M.L., Shadid, J., Shafaat, O., Shahabi, S., Shaheen, A.A., Shaikh, M.A., Shalash, A.S., Shams-Beyranvand, M., Shamsizadeh, M., Sharafi, K., Sheikh, A., Sheikhtaheri, A., Shibuya, K., Shield, K.D., Shigematsu, M., Shin, J.I., Shin, M.-J., Shiri, R., Shirkoohi, R., Shuval, K., Siabani, S., Sierpinski, R., Sigfusdottir, I.D., Sigurvinsdottir, R., Silva, J.P., Simpson, K.E., Singh, J.A., Singh, P., Skiadaresi, E., Skou, S.T., Skryabin, V.Y., Smith, E.U.R., Soheili, A., Soltani, S., Soofi, M., Sorensen, R.J.D., Soriano, J.B., Sorrie, M.B., Soshnikov, S., Soyiri, I.N., Spencer, C.N., Spotin, A., Sreeramareddy, C.T., Srinivasan, V., Stanaway, J.D., Stein, C., Stein, D.J., Steiner, C., Stockfelt, L., Stokes, M.A., Straif, K., Stubbs, J.L., Sufiyan, M.a.B., Suleria, H.A.R., Suliankatchi Abdulkader, R., Sulo, G., Sultan, I., Szumowski, Ł., Tabarés-Seisdedos, R., Tabb, K. M., Tabuchi, T., Taherkhani, A., Tajdini, M., Takahashi, K., Takala, J.S., Tamiru, A. T., Taveira, N., Tehrani-Banihashemi, A., Temsah, M.-H., Tesema, G.A., Tessema, Z. T., Thurston, G.D., Titova, M.V., Tohidinik, H.R., Tonelli, M., Topor-Madry, R., Topouzis, F., Torre, A.E., Touvier, M., Tovani-Palone, M.R.R., Tran, B.X., Travillian, R., Tsatsakis, A., Tudor Car, L., Tyrovolas, S., Uddin, R., Umeokonkwo, C. D., Unnikrishnan, B., Upadhyay, E., Vacante, M., Valdez, P.R., van Donkelaar, A., Vasankari, T.J., Vasseghian, Y., Veisani, Y., Venketasubramanian, N., Violante, F.S., Vlassov, V., Vollset, S.E., Vos, T., Vukovic, R., Waheed, Y., Wallin, M.T., Wang, Y., Wang, Y.-P., Watson, A., Wei, J., Wei, M.Y.W., Weintraub, R.G., Weiss, J., Werdecker, A., West, J.J., Westerman, R., Whisnant, J.L., Whiteford, H.A., Wiens, K. E., Wolfe, C.D.A., Wozniak, S.S., Wu, A.-M., Wu, J., Wulf Hanson, S., Xu, G., Xu, R., Yadgir, S., Yahyazadeh Jabbari, S.H., Yamagishi, K., Yaminfirooz, M., Yano, Y., Yaya, S., Yazdi-Feyzabadi, V., Yeheyis, T.Y., Yilgwan, C.S., Yilma, M.T., Yip, P., Yonemoto, N., Younis, M.Z., Younker, T.P., Yousefi, B., Yousefi, Z., Yousefinezhadi, T., Yousuf, A.Y., Yu, C., Yusefzadeh, H., Zahirian Moghadam, T., Zamani, M., Zamanian, M., Zandian, H., Zastrozhin, M.S., Zhang, Y., Zhang, Z.-J., Zhao, J.T., Zhao, X.-J.G., Zhao, Y., Zhou, M., Ziapour, A., Zimsen, S.R.M., Brauer, M., Afshin, A., Lim, S.S., 2020. Global burden of 87 risk factors in 204 countries and territories, 1990–2019: a systematic analysis for the global burden of disease study 2019. Lancet 396, 1223–1249. https://doi.org/10.1016/S0140-6736(20)30752-2.

Paraskevopoulou, D., Bougiatioti, A., Stavroulas, I., Fang, T., Lianou, M., Liakakou, E., Gerasopoulos, E., Weber, R., Nenes, A., Mihalopoulos, N., 2019. Yearlong variability of oxidative potential of particulate matter in an urban Mediterranean environment. Atmos. Environ. 206, 183–196. https://doi.org/10.1016/j.atmosenv.2019.02.027.

Puthussery, J.V., Dave, J., Shukla, A., Gaddamidi, S., Singh, A., Vats, P., Salana, S., Ganguly, D., Rastogi, N., Tripathi, S.N., Verma, V., 2022. Effect of biomass burning, diwali fireworks, and polluted fog events on the oxidative potential of fine ambient particulate matter in Delhi, India. Environ. Sci. Technol. 56, 14605–14616. https://doi.org/10.1021/acs.est.2c02730.

Qin, L., Yang, L., Liu, L., Tong, S., Liu, Q., Li, G., Zhang, H., Zhu, W., Liu, G., Zheng, M., Jiang, G., 2024. Oxidative potential and persistent free radicals in dust storm particles and their associations with hospitalization. Nat. Commun. 15, 10827. https://doi.org/10.1038/s41467-024-55151-8.

Reff, A., Bhave, P.V., Simon, H., Pace, T.G., Pouliot, G.A., Mobley, J.D., Houyoux, M., 2009. Emissions inventory of $PM_{2.5}$ trace elements across the United States. Environ. Sci. Technol. 43, 5790–5796. https://doi.org/10.1021/es802930x.

Salana, S., Yu, H., Dai, Z., Subramanian, P.S.G., Puthussery, J.V., Wang, Y., Singh, A., Pope, F.D., Leiva G, M.A., Rastogi, N., Tripathi, S.N., Weber, R.J., Verma, V., 2024. Inter-continental variability in the relationship of oxidative potential and cytotoxicity with $PM_{2.5}$ mass. Nat. Commun. 15, 5263. https://doi.org/10.1038/s41467-024-49649-4.

Schwartz, J., Laden, F., Zanobetti, A., 2002. The concentration-response relation between PM(2.5) and daily deaths. Environ. Health Perspect. 110, 1025–1029. https://doi.org/10.1289/ehp.021101025.

Shang, J., Zhang, Y., Schauer, J.J., Chen, S., Yang, S., Han, T., Zhang, D., Zhang, J., An, J., 2022. Prediction of the oxidation potential of PM2.5 exposures from pollutant composition and sources. Environ. Pollut. 293, 118492. https://doi.org/10.1016/j.envpol.2021.118492.

Shen, G., Tao, S., Wei, S., Chen, Y., Zhang, Y., Shen, H., Huang, Y., Zhu, D., Yuan, C., Wang, H., Wang, Y., Pei, L., Liao, Y., Duan, Y., Wang, B., Wang, R., Lv, Y., Li, W., Wang, X., Zheng, X., 2013. Field measurement of emission factors of PM, EC, OC, parent, Nitro-, and Oxy- polycyclic aromatic hydrocarbons for residential briquette, coal cake, and wood in rural Shanxi, China. Environ. Sci. Technol. 47, 2998–3005. https://doi.org/10.1021/es304599g.

Shen, J., Taghvaee, S., La, C., Oroumiyeh, F., Liu, J., Jerrett, M., Weichenthal, S., Del Rosario, I., Shafer, M.M., Ritz, B., Zhu, Y., Paulson, S.E., 2022. Aerosol oxidative potential in the greater Los Angeles area: source apportionment and associations with socioeconomic position. Environ. Sci. Technol. 56, 17795–17804. https://doi.org/10.1021/acs.est.2c02788.

Shiraiwa, M., Ueda, K., Pozzer, A., Lammel, G., Kampf, C.J., Fushimi, A., Enami, S., Arangio, A.M., Fröhlich-Nowoisky, J., Fujitani, Y., Furuyama, A., Lakey, P.S.J., Lelieveld, J., Lucas, K., Morino, Y., Pöschl, U., Takahama, S., Takami, A., Tong, H., Weber, B., Yoshino, A., Sato, K., 2017. Aerosol health effects from molecular to global scales. Environ. Sci. Technol. 51, 13545–13567. https://doi.org/10.1021/acs.est.7b04417.

Strak, M., Janssen, N., Beelen, R., Schmitz, O., Vaartjes, I., Karssenberg, D., van den Brink, C., Bots, M.L., Dijst, M., Brunekreef, B., Hoek, G., 2017. Long-term exposure to particulate matter, NO_2 and the oxidative potential of particulates and diabetes prevalence in a large national health survey. Environ. Int. 108, 228–236. https://doi.org/10.1016/j.envint.2017.08.017.

Verma, P.K., Devaprasad, M., Dave, J., Meena, R., Bhowmik, H., Tripathi, S.N., Rastogi, N., 2024. Summertime oxidative potential of atmospheric $PM_{2.5}$ over New Delhi: effect of aerosol ageing. Sci. Total Environ. 920, 170984. https://doi.org/10.1016/j.scitotenv.2024.170984.

Wang, W., Cao, G., Zhang, J., Chen, Z., Dong, C., Chen, J., Cai, Z., 2022. p-Phenylenediamine-Derived quinones as new contributors to the oxidative potential of fine particulate matter. Environ. Sci. Technol. Lett. 9, 712–717. https://doi.org/10.1021/acs.estlett.2c00484.

Weichenthal, S., Lavigne, E., Traub, A., Umbrio, D., You, H., Pollitt, K., Shin, T., Kulka, R., Stieb, D.M., Korsiak, J., Jessiman, B., Brook, J.R., Hatzopoulou, M., Evans, G., Burnett, R.T., 2021. Association of sulfur, transition metals, and the oxidative potential of outdoor $PM_{2.5}$ with acute cardiovascular events: a case-crossover Study of Canadian adults. Environ. Health Perspect. 129, 107005. https://doi.org/10.1289/EHP9449.

Weichenthal, S., Shekarrizfard, M., Traub, A., Kulka, R., Al-Rijleh, K., Anowar, S., Evans, G., Hatzopoulou, M., 2019. Within-city spatial variations in multiple measures of $PM_{2.5}$ oxidative potential in Toronto, Canada. Environ. Sci. Technol. 53, 2799–2810. https://doi.org/10.1021/acs.est.8b05543.

Weichenthal, S.A., Lavigne, E., Evans, G.J., Godri Pollitt, K.J., Burnett, R.T., 2016. Fine particulate matter and emergency room visits for respiratory illness. Effect modification by oxidative potential. Am. J. Respir. Crit. Care Med. 194, 577–586. https://doi.org/10.1164/rccm.201512-2434OC.

Wu, D., Zheng, H., Li, Q., Jin, L., Lyu, R., Ding, X., Huo, Y., Zhao, B., Jiang, J., Chen, J., Li, X., Wang, S., 2022. Toxic potency-adjusted control of air pollution for solid fuel combustion. Nat. Energy 7, 194–202. https://doi.org/10.1038/s41560-021-00951-1.

Xing, C., Wang, Y., Yang, X., Zeng, Y., Zhai, J., Cai, B., Zhang, A., Fu, T.-M., Zhu, L., Li, Y., Wang, X., Zhang, Y., 2023. Seasonal variation of driving factors of ambient $PM_{2.5}$ oxidative potential in Shenzhen, China. Sci. Total Environ. 862, 160771. https://doi.org/10.1016/j.scitotenv.2022.160771.

Yao, K., Xu, Y., Zheng, H., Zhang, X., Song, Y., Guo, H., 2024. Oxidative potential associated with reactive oxygen species of size-resolved particles: the important role of the specific sources. J. Environ. Manag. 360, 121122. https://doi.org/10.1016/j.jenvman.2024.121122.

Zauli-Sajani, S., Thunis, P., Pisoni, E., Bessagnet, B., Monforti-Ferrario, F., De Meij, A., Pekar, F., Vignati, E., 2024. Reducing biomass burning is key to decrease $PM_{2.5}$ exposure in European cities. Sci. Rep. 14, 10210. https://doi.org/10.1038/s41598-024-60946-2.

Zhang, L., Hu, X., Chen, S., Chen, Y., Lian, H.-Z., 2023a. Characterization and source apportionment of oxidative potential of ambient $PM_{2.5}$ in Nanjing, a megacity of Eastern China. Environ. Pollut. Bioavailab. 35, 2175728. https://doi.org/10.1080/26395940.2023.2175728.

Zhang, X., Chen, X., Yue, Y., Wang, S., Zhao, B., Huang, X., Li, T., Sun, Q., Wang, J., 2023b. Ecological study on global health effects due to source-specific ambient fine particulate matter exposure. Environ. Sci. Technol. 57, 1278–1291. https://doi.org/10.1021/acs.est.2c06752.

Zhang, Y., Tian, J., Wang, Q., Qi, L., Manousakas, M.I., Han, Y., Ran, W., Sun, Y., Liu, H., Zhang, R., Wu, Y., Cui, T., Daellenbach, K.R., Slowik, J.G., Prévôt, A.S.H., Cao, J., 2023c. High-time-resolution chemical composition and source apportionment of $PM_{2.5}$ in northern Chinese cities: implications for policy. Atmos. Chem. Phys. 23, 9455–9471. https://doi.org/10.5194/acp-23-9455-2023.

Zhao, S., Tian, H., Luo, L., Liu, H., Wu, B., Liu, S., Bai, X., Liu, W., Liu, X., Wu, Y., Lin, S., Guo, Z., Lv, Y., Xue, Y., 2021. Temporal variation characteristics and source apportionment of metal elements in $PM_{2.5}$ in urban Beijing during 2018–2019. Environ. Pollut. 268, 115856. https://doi.org/10.1016/j.envpol.2020.115856.